Pontifícia Universidade Católica
do Rio de Janeiro

Camila Nunes Metello

Analytical representation of immediate cost functions in SDDP

DISSERTAÇÃO DE MESTRADO

Dissertation presented to the Programa de Pós-Graduação em Engenharia Elétrica of the Departamento de Engenharia Elétrica, PUC-Rio as partial fulfillment of the requirements for the degree of Mestre em Engenharia Elétrica.

Advisor: Prof. Reinaldo Castro Souza
Co-Advisor: Dr. Mario Veiga Ferraz Pereira

Rio de Janeiro
August 2016

PONTIFÍCIA UNIVERSIDADE CATÓLICA
DO RIO DE JANEIRO

Camila Nunes Metello

Analytical representation of immediate cost functions in SDDP

DISSERTAÇÃO DE MESTRADO

Dissertation presented to the Programa de Pós-Graduação em Engenharia Elétrica of the Departamento de Engenharia Elétrica do Centro Técnico Científico da PUC-Rio, as partial fulfillment of the requeriments for the degree of Mestre.

Prof. Reinaldo Castro Souza
Advisor
Departamento de Engenharia Elétrica – PUC-Rio

Dr. Mario Veiga Ferraz Pereira
Co-Advisor
PSR Soluções e Consultoria em Energia Ltada

Dr. Geraldo Gil Veiga
RN Tecnologia

Profa. Fernanda Souza Thomé
PSR Soluções e Consultoria em Energia

Prof. Márcio da Silveira Carvalho
Coordinator of the Centro Técnico
Científico da PUC-Rio

Rio de Janeiro, August 15th, 2016

Camila Nunes Metello

Received the B.Sc. degree (2014) in industrial engineering and the M.Sc. degree (2016) in operations research from Pontifical Catholic University of Rio de Janeiro (PUC-Rio), Rio de Janeiro, Brazil. She is currently working at PSR consulting company in the development and maintenance of software focused in operation and planning of power systems.

Bibliographic data

Metello, Camila Nunes

Analytical representation of immediate cost functions in SDDP / Camila Nunes Metello; advisor: Reinaldo Castro Souza; co-advisor: Mario Veiga Ferraz Pereira. – 2016.

82 f. : il. color. ; 30 cm

Dissertação (mestrado) – Pontifícia Universidade Católica do Rio de Janeiro, Departamento de Engenharia Elétrica, 2016.

Inclui bibliografia

1. Engenharia elétrica – Teses. 2. Despacho. 3. PDDE. 4. Programação matemática. I. Souza, Reinaldo Castro. II. Pereira, Mario Veiga Ferraz. III. Pontifícia Universidade Católica do Rio de Janeiro. Departamento de Engenharia Elétrica. IV. Título.

CDD: 621.3

Acknowledgments

First, I would like to thank my parents, Adélia and Guilherme, for every lesson, incentive and support I have ever received in my life. I would not have done it without you. I would also like to thank:

My advisor, Reinaldo Souza, for his smart remarks and support.

My co-advisor, Mario Veiga, who I look up to very much. Thank you so much for dedicating so much time in my professional development. You have always believed in me and this was so important to me.

To my friends at PSR: Joaquim Garcia, Rafael Kelman, Luiz Carlos, Fernanda Thomás, Sergio Granville, Julio Alberto and my friend Tiago Andrade. You were amazing through all my journey.

To my friends and family, who were always ready to offer help.

Finally, I would like to thank DEE for the opportunity and trust for taking me into the Masters program and CAPES, for giving me an exemption scholarship.

Abstract

Metello, Camila Nunes; Castro Souza, Reinaldo (Advisor); Pereira, Mario Veiga Ferraz (Co-advisor). **Analytical representation of immediate cost functions in SDDP.** Rio de Janeiro, 2016. 82p. MSc. Dissertation – Departamento de Engenharia Elétrica, Pontifícia Universidade Católica do Rio de Janeiro.

The increasing penetration of renewable generation plants in electric systems, combined with the development of effective short-term energy storage batteries, demand scheduling to be represented on an hourly basis or even in smaller time intervals. Multistage stochastic optimization in such time resolution would imply in the increase of the problem's dimension, which might result in the impossibility of solving such problems. This work presents a method that is able to take into account such small time intervals while avoiding the considerable increase of computational effort. This method consists in calculating the analytical representation of the immediate cost function that is applied in the context of stochastic dual dynamic programming (SDDP). The function represents immediate operation costs as a function of the total hydroelectric generation optimal decision. As the immediate cost function is piecewise linear, it leads to a structure very similar to the one used to approximate the future cost function (cut sets). Results of the application of the method in real electric systems are presented.

Keywords

Scheduling; SDDP; Mathematical programming.

Resumo

Metello, Camila Nunes; Castro Souza, Reinaldo (Orientador); Pereira, Mario Veiga Ferraz (Co-orientador). **Representação analítica da função de custo imediato no SDDP.** Rio de Janeiro, 2016. 82p. Dissertação de Mestrado – Departamento de Engenharia Elétrica, Pontifícia Universidade Católica do Rio de Janeiro.

A penetração crescente de geração de energia renovável combinada com o desenvolvimento de baterias eficazes, capazes de estocar energia no curto prazo, demandam a representação horária (ou até sub horária) de modelos de despacho de operação. A necessidade de representar intervalos de tempo tão curtos implicaria no aumento significativo da dimensão do problema, possivelmente o tornando intratável computacionalmente. Nesta dissertação, é proposto um método capaz de levar em consideração tais pequenos intervalos de tempo, evitando o aumento considerável de esforço computacional para problemas de despacho hidrotérmico. Este método consiste em calcular a representação analítica da função custo imediato que é então aplicada no contexto de programação dinâmica dual estocástica (SDDP). A função representa os custos operativos imediatos em função da decisão ótima de geração hidrelétrica total. Como a função de custo imediato é linear por partes, ela possui estrutura muito semelhante à utilizada para aproximar a função de custo futuro (conjunto de cortes). São apresentados resultados da aplicação do método em sistemas de energia reais.

Palavras-chave

Despacho; PDDE; Programação matemática.

Contents

List de figures

List de tables

List of Abreviations

DP – *Dynamic Programming*
FCF – *Future Cost Function*
HPC – *Hydrothermal Production Costing*
ICF – *Immediate Cost Function*
LDC – *load duration curve*
PPC – *Probabilistic Production Costing*
SDDP – *Stochastic Dual Dynamic Programming*
SDP – *Stochastic Dynamic Programming*

NOTATION

Indexes

$i = 1, \ldots, I$ hydro plants

$j = 1, \ldots, J$ thermal plants

$p = 1, \ldots, P$ hyperplanes (Benders cuts) in the future cost function

$r = 1, \ldots, R$ electrical areas

$t = 1, \ldots, T$ time stages (typically weeks or months)

$\tau = 1, \ldots, \mathcal{T}$ intra-stage time intervals (e.g. peak/medium/low demand or 168 hours in a week)

U_i set of hydro plants immediately upstream of plant i

$l = 1, \ldots, L$ hyperplanes (Benders cuts) in the immediate cost function

Ω_r set of hydro plants in area r

Θ_r set of thermal plants in area r

Decision variables for the operation problem in stage t

$v_{t+1,i}$ stored volume of hydro i by the end of stage t

$u_{t,i}$ turbined volume of hydro i stage t

$\nu_{t,i}$ spilled volume of hydro i in stage t

$e_{t,\tau,i}$ generation of hydro i in time interval τ, stage t

$e_{t,i}$ generation of hydro i in stage t

$e_{t,r}$ total hydro generation in area r in stage t

$g_{t,\tau,j}$ generation of thermal plant j in time interval τ, stage t

$f_{t,\tau}^{q,r}$ power flow from area q to area r in time interval τ, stage t

α_{t+1} present value of expected future cost from $t+1$ to T

β_t present value of immediate cost at stage t

Known values for the operation problem in stage t

$\hat{a}_{t,i}$ lateral inflow to hydro i in stage t

$\overline{u}_i$ maximum turbined outflow of hydro i

$\hat{v}_{t,i}$ stored volume of hydro i in the beginning of stage t

$\overline{v}_i$ maximum storage of hydro i

ρ_i production coefficient of hydro i

$\overline{e}_i$ maximum energy generation of hydro i

c_j variable operating cost of thermal plant j

$\overline{g}_j$ maximum generation of thermal plant j

$\hat{\delta}_{t,\tau}$ residual load (load - renewable generation) in time interval τ, stage t

$\overline{f}^{q,r}$ maximum power flow between areas q and r

Benders cut coefficients - Future Cost Function

$\hat{\phi}^p_{t+1,i}$ coefficient of cut p for hydro plant i's storage, $v_{t+1,i}$

$\hat{\sigma}^p_{t+1}$ constant term

Immediate Cost Function

$\hat{\mu}^l_{t,i}$ coefficient of cut l for hydroelectric generation i , $e_{t,q}$

$\hat{\Delta}^l_t$ constant term of cut l

$\hat{e}^k_t$ total hydroelectric generation in area q, stage t, discretizarion k

$\hat{\beta}^k_t$ immediate cost in stage t, discretization k

Multipliers

$\pi^h_{t,i}$ multiplier associated to the water balance equations of hydroelectric plant i in stage t

$\pi^{\alpha p}_{t,i}$ multipliers associated to the future cost function constraint of hydroelectric plant i in stage t

1
Introduction

1.1
Hydrothermal system generation

Historically, hydroelectricity has been the most important renewable energy source and, in many countries, also the most economic option. Even today, despite the explosive growth of wind, solar and biomass, renewable energy is still dominated by hydropower. For instance, a recent World Bank survey (31) (2013) on hydroelectric penetration shows several countries in which hydroelectric generation has a significant importance in total energy generation: Iceland(71%),Colombia(68.5%), Brazil (68%), Canada(60%) and several others.

It is also well-known (32) that scheduling the production and planning the capacity expansion of systems with a significant hydro share is a complex problem due to two features of this source: (i) energy storage in the reservoirs; and (ii) high variability of inflows to hydro plants. The storage feature (i) means that it is not possible to determine the least-cost operation of a hydrothermal system without assessing the tradeoff between using hydropower now – and thus avoiding some thermal generation costs – or storing the water for future use, when the thermal cost savings could be higher. This time coupling makes hydrothermal operation much more complex than that of purely thermal systems, where the optimal scheduling for each time stage can be determined independently of the next stages [1]. The problem complexity is compounded by feature (ii), inflow variability. The reason is that uncertainty about future inflows means that the tradeoff between immediate and future use of hydropower has to be evaluated probabilistically, that is, for each branch of a "tree" of future inflow scenarios. Figure 1.1 illustrates the so-called "operator's dilemma" for a toy system composed of two time stages and two future inflow scenarios.

[1] Thermal restrictions such as unit commitment and ramp constraints only create short-term dependency

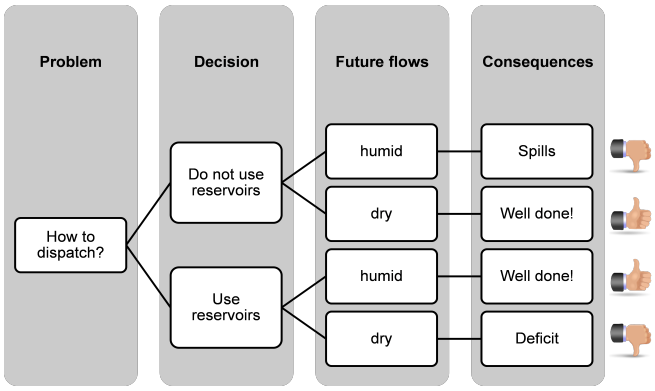

Figure 1.1: Dispatch uncertainty decision making problem

In this toy system, we could calculate the operating cost for each alternative decision and inflow scenario and select the one that results in the smallest expected operation cost. In real life, however, this tree is very large. In Brazil, for example, there are 30 inflow scenarios per month (12), which means that the number of nodes is 30^T, where T represents the future months that can be affected by an operating decision today ("horizon of influence"). Intuitively the horizon of influence increases with the hydro storage capacity. In the case of Brazil, which due to its topography has very large reservoirs, T is 60 months (five years) (12). As a consequence, the scenario tree that the Brazil's National System Operator (ONS) has to evaluate has $30^{60} \approx 10^{88}$ nodes, more than the number of particles (electrons, photons etc.) in the observable universe.

Because of this combination of economic importance and methodological complexity, optimizing the operation and planning of hydrothermal systems has always been a pioneering area for the application of advanced stochastic optimization techniques. In particular, stochastic dynamic programming (SDP), described in (7) and (30) (See Appendix A for more details) and more recent improvements such as stochastic dual dynamic programming (SDDP) (24) and (23) , approximate dynamic programming (ADP) (25) and others, have been widely applied to real-life systems for decades.

In this work, we propose an extension of the SDDP algorithm, which is one of the most widely applied for hydrothermal scheduling worldwide. Appendix B describes the SDDP scheme in detail.

1.1.1 Immediate and future cost functions

All stochastic DP-based algorithms decompose the multistage optimization problem into a sequence of one-stage operation problems, where the stage is typically a month, or a week, and the objective is to determine the hydro

production schedule that minimizes the total cost given by the sum of two functions: immediate cost and expected future cost of supplying the load. As their names imply, these functions represent the trade-off between using the hydro production now and storing the water for use in the future.

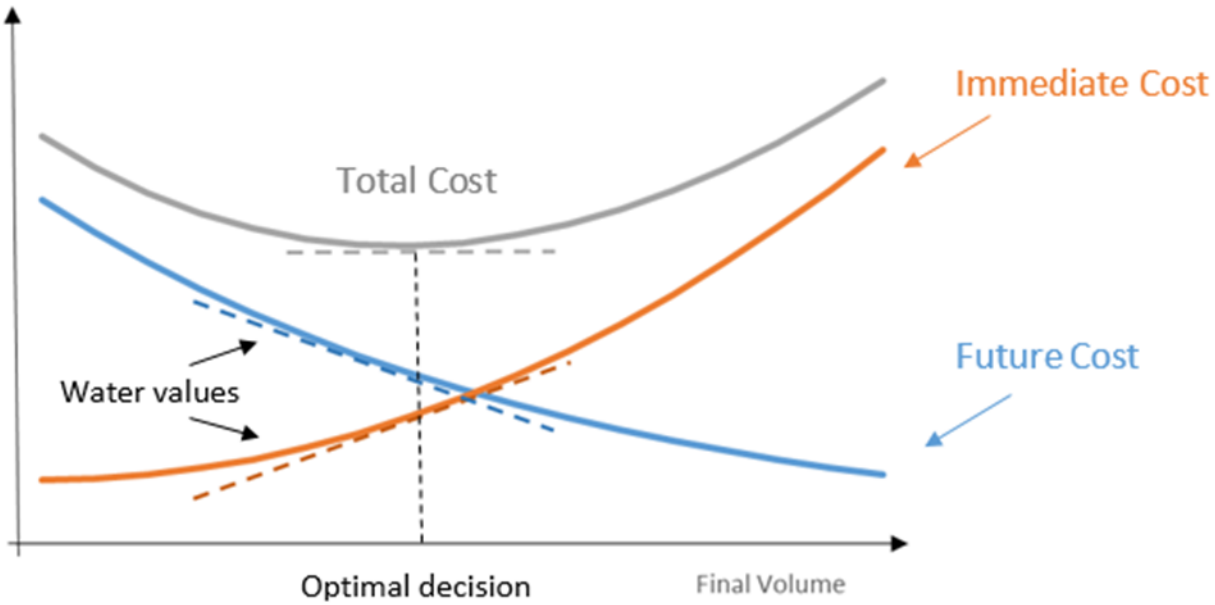

Figure 1.2: Immediate and future cost functions

The immediate cost function (ICF) provides the least-cost dispatch, i.e., the minimum thermal fuel cost of supplying the residual demand (load – hydro production) along the current stage. As figure 1.2 shows, the ICF increases as the amount of storage left for the next stage also increases. In turn, the future cost function (FCF) is related to the expected use of hydropower in the future stages and scenarios. As expected, the FCF goes in the opposite direction of the ICF, decreasing with the final storage.

If the ICF and FCF had the simple shapes of the above figure, it would be easy to see that the optimal solution of $Min\ ICF(v) + FCF(v)$ would be the volume v^* that equalizes the function derivatives, i.e. $\frac{\partial ICF(v)}{\partial v} = -\frac{\partial FCF(v)}{\partial v} for\ v = v^*$. In hydropower scheduling, these derivatives are known as the immediate and future *water values*, because they represent the *opportunity costs* of using the water now or storing it for the future. As a consequence, the optimality condition may be interpreted as the following operational logic: if the future water value is higher than the immediate one $\left(|\frac{\partial FCF(v)}{\partial v}| > \frac{\partial ICF(v)}{\partial v}\right)$, we store one additional unit of water. The result of this action is to increase the immediate water value (less water available) and, conversely, to decrease the future's (more water). As a consequence, the two water values become closer

$\left(|\frac{\partial FCF(v)}{\partial v}| \approx \frac{\partial ICF(v)}{\partial v}\right)$. The process continues until there is no net economic benefit of increasing storage, which is the optimality condition.

It will also be seen in this work how to calculate the hydroelectric opportunity costs ($/MWh), obtained by dividing water values by the hydro's production factor. In particular, the fact that opportunity costs are equal at the optimal solution will be one of the key hypothesis in our proposed methodology.

For all stochastic DP algorithms the ICF is represented *implicitly* through the equations and constraints of the least-cost dispatch mentioned above. In turn, the FCF is built through a so-called *backward recursion* in which one-stage operation problems are successively solved from the last to the first stage. The essential difference between these algorithms proposed so far is on the methods for building the FCF and the simplifying assumption.

A second key concept of our proposed methodology is to build an explicit ICF as a piecewise linear function.

1.2 One-stage operation problem in SDDP

The SDDP time stage is typically a week, or month, which is indexed by $t = 1, \ldots, T$. In each stage, there are $\tau = 1, \ldots, \mathcal{T}$ intra-stage time intervals, representing, for example, the 730 hours in a month or, as it will be seen later, aggregated load blocks, for example high, medium and low load levels. Next, we formulate, without loss of generality, a simplified version (no network representation, no variable hydro production factor, etc.) of the SDDP operation problem in stage t.

Objective function

The objective is to minimize the total cost α_t given by immediate and future costs. The immediate cost is represented by the sum of thermal generation costs $c_j \times g_{t,\tau,j}$ along the intra-stage time intervals $\tau = 1, \ldots, \mathcal{T}$. In turn, the future cost is represented by the function $\alpha_{t+1}(v_{t+1})$, which will be detailed later.

$$\alpha_t(\hat{v}_t) = Min \sum_j c_j \sum_\tau g_{t,\tau.j} + \alpha_{t+1}(v_{t+1}) \tag{1-1}$$

Where $\hat{v}_t$ is the storage at the beginning of stage t ($\hat{}$ indicates a known value), $j \in J$ are indexes the thermal plants, c_j is the variable operating cost

of thermal plant j and $g_{t,\tau,j}$ is the energy generation of thermal plant j in block τ, stage t.

Water balance for each stage

The next set of equations represents the storage variation in the system reservoirs: the final storage is equal to initial storage plus the inflow along the stage (lateral inflow plus outflows from the upstream plants) minus the plant's outflow (turbined and spilled).

$$v_{t+1,i} = \hat{v}_{t,i} + \hat{a}_{t,i} + \sum_{m \in U_i} (u_{t,m} + \nu_{t,m}) - u_{t,i} - \nu_{t,i}, \forall i \in I \tag{1-2}$$

Where $i \in I$ are the indexes the hydro plants, $v_{t+1,i}$ is the stored volume of hydro i by the end of stage t, $\hat{v}_{t,i}$ is the stored volume of hydro i in the beginning of stage t, $\hat{a}_{t,i}$ is the lateral inflow to hydro i in stage t, $u_{t,i}$ is the turbined volume of hydro i stage t, $\nu_{t,i}$ is the spilled volume of hydro i in stage t and $m \in U_i$ is the set of hydro plants immediately upstream of plant i.

It is important to observe that in this formulation the water balance is carried out for the entire stage, not for each intra-stage time interval. That is, we assume that the hydro storage is large enough to accommodate any intra-stage variation in the hydro production schedule.

This assumption is consistent with the fact that the reservoir storage is represented as a state variable in the stochastic DP recursion, i.e. that there is a meaningful tradeoff between using the water in stage t or storing it for future use. It is also the operational reality in the 70 countries where SDDP has been applied (we will show later how smaller reservoirs with regulation horizons smaller than the stage duration can be represented by the methodology proposed in this work).

Storage and turbined outflow limits

$$v_{t+1,i} \leq \overline{v}_i, \forall i \in I \tag{1-3}$$

$$u_{t,i} \leq \overline{u}_i, \forall i \in I \tag{1-4}$$

Where $\overline{v}_i$ is the maximum storage of hydro i and $\overline{u}_i$ is the maximum turbined outflow of hydro i.

Hydro generation

In this set of constraints, the total hydro generation for stage t, $e_{t,i}$, is obtained from the turbined outflow $u_{t,i}$. This total hydro generation is then disaggregated into a generation schedule $e_{t,\tau,i}$ for each interval τ.

$$e_{t,i} = \rho_i u_{t,i}, \forall i \in I \tag{1-5}$$

$$\sum_{\tau} e_{t,\tau,i} = e_{t,i}, \forall i \in I \tag{1-6}$$

$$e_{t,\tau,i} \leq \overline{e}_i, i \in I \tag{1-7}$$

Where ρ_i is the production coefficient (kWh/m^3) of hydro i and $\overline{e}_i$ is the maximum energy generation of hydro i.

Load supply for each intra-stage interval

The sum of hydro plus thermal generation is equal to the residual load demand minus renewable generation.

$$\sum_{i} e_{t,\tau,i} + \sum_{j} g_{t,\tau,j} = \hat{\delta}_{t,\tau}, \forall \tau \in \mathcal{T} \tag{1-8}$$

$$g_{t,\tau,j} \leq \overline{g}_j, \forall \tau \in \mathcal{T} \tag{1-9}$$

Where $\hat{\delta}_{\tau,t}$ is the residual load (load - renewable generation) of time τ, stage t and $\overline{g}_j$ is the maximum generation of thermal plant j.

Future cost function

In the SDDP scheme, the future cost function is represented by a set of hyperplanes

$$\alpha_{t+1} \geq \sum_{i} \hat{\phi}^{p}_{t+1,i} \times v_{t+1,i} + \hat{\sigma}^{p}_{t+1}, \forall p \in P \tag{1-10}$$

Where $p \in P$ are the hyperplanes (Benders cuts) in the future cost function, $\hat{\phi}^{p}_{t+1,i}$ is the coefficient of cut p for hydro plant i's storage, $v_{t+1,i}$ and $\hat{\sigma}^{p}_{t+1}$ is the constant term of cut p.

Appendix B describes the calculation of the hyperplane coefficients $\hat{\phi}^{p}_{t+1,i}$ and constant term $\hat{\sigma}^{p}_{t+1}$.

1.3 Solution of the one-stage operation problem

The operation problem (1-1 - 1-10) is a linear programming (LP) problem and, thus, can be solved by any available commercial optimization software. However, computational efficiency is important because this problem has to be solved a very large number of times in the SDDP scheme: T (number of time stages) $\times$ K (SDDP iterations) $\times$ S (scenarios in SDDP's forward step) $\times$ L (number of conditioned inflow scenarios in SDDP's backward step).

1.3.1 Managing the number of operation problems

As an illustration, the SDDP-based Monthly Operation Plan (PMO) (12) calculated by Brazil's National System Operator (ONS) has T=120; K=25; S=2000; L=20, which results in 126 million LPs. Fortunately, the SDDP algorithm is very suitable for distributed processing techniques (shown in appendix B), which has allowed the solution of large scale systems such as Brazil's in a reasonable amount of time. Using PSR's SDDP model (26), the PMO case takes around 90 minutes (using 16 processors).(19) also presented a study on the efficiency of SDDP parallelization.

1.3.2 Improving the solution time of each operation problem

In the distributed processing scheme, each "grain" is the solution of a one-stage operation problem (1-1 - 1-10). This means that a reduction in the individual LP solution time has a direct impact on the total solution time, which has motivated the investigation of customized LP solution schemes. As usual, the starting point for these investigations is the structure of the problem variables and constraints. As seen, the operation problem is composed of the following sets of constraints (ignoring bounds): (i) water balance and hydro generation equations: 2×I; (ii) power balance equations: $\mathcal{T}$ (number of time intervals); (iii) future cost function (FCF): K (SDDP iterations) ×S (scenarios in the probabilistic simulations) hyperplanes. For the same Brazilian PMO example (considering the individualized representation of the hydroelectric plants), we have: (i) 2×I (=130)=260; (ii) $\mathcal{T}$=730 (assuming monthly hourly intervals); and (iii) K(=25) × S(=2000)=50,000.

In turn, the LP variables are: (a) hydro-related (final storage, turbined and spilled outflow per stage): 3×I; and (b) power-related (hydro and thermal generation per time interval): $\mathcal{T}$×(I+J). For the PMO example, we have: (a) 3×I (=130)=390; and (b) $\mathcal{T}$ (=730)×(I (=130)+J (=150))=204,400.

1.3.3
Relaxation schemes for the FCF

Initially, we observe that the constraints are dominated by the 50,000 FCF hyperplanes. However, we know from experience that only a few of those hyperplanes will be binding at the optimal solution. As a consequence, relaxation schemes with dual simplex steps were shown to be very effective, requiring only 5 to 10 hyperplanes to be added.

A third key concept of our work is to apply the same effective relaxation techniques to the proposed analytical immediate cost function.

1.3.4
Aggregation of time intervals

Given that the FCF constraints can be handled by relaxation, the next "bottleneck" is the number of intra-stage time intervals $\mathcal{T}$. For the Brazilian system, for example, solving a problem with 730 intervals may take 400 times longer than solving for only one block (that is, the average load).

Historically, the solution has been to *aggregate* the hourly intervals into load blocks, for example, high, medium and low load levels. Figure 1.3 illustrates a popular aggregation technique, in which the hourly loads are ordered from highest to lowest and then aggregated into clusters (three, in this case), widely known as load duration curve (LDC).

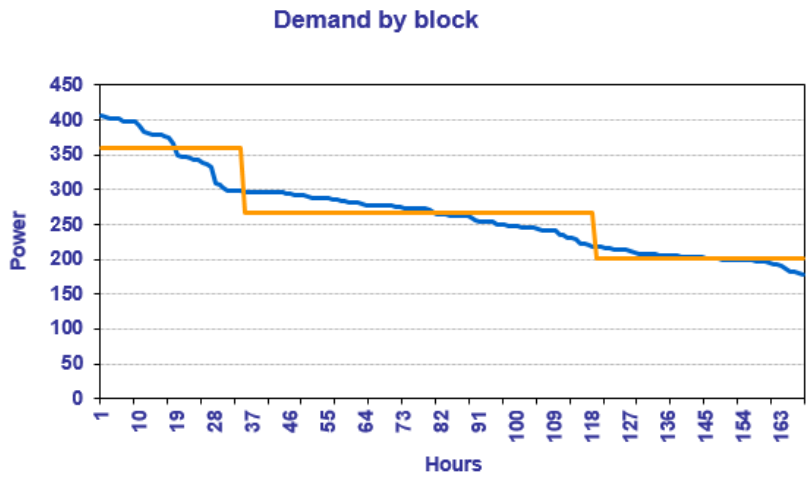

Figure 1.3: Example of transformation of hourly load curve into a load duration curve with 3 blocks

1.4 Motivation for this work

The use of load duration curves, together with distributed processing techniques, has allowed a significant reduction of SDDP's computational effort without loss of accuracy. This, in turn, has contributed significantly to the successful application of stochastic optimization techniques to the operation and planning of large-scale systems for the past several years.

More recently, however, the worldwide growth of renewable generatioan such as wind, biomass and solar has led to concerns about the accuracy of using load duration curves in probabilistic operation and planning. The reason is that the energy produced by those new resources may vary substantially in very short intervals.

For this reason, the analysis of renewable insertion is usually carried out with hourly intervals, or even shorter, 5-15 minutes.

At first sight, the clustering technique of figure 3 could still be used, only applied now to the *residual load*, i.e., subtracted from the renewable production. The computational effort would be higher because the renewable production in SDDP – and hence the net load – may be different for each stage and scenario, but still, it would be much smaller than representing the hourly load. However, this approach has two potential drawbacks: (i) differently from loads, which usually have a strong spatial correlation (i.e. the peak hours in different regions tend to coincide, and so on), renewable production is much more dispersed. As a consequence, the clustering of residual loads in multiple regions becomes more complex and less accurate; (ii) by construction, the clustering scheme cannot represent the chronological evolution of energy production, which is an important feature in the case of renewables because the chronological sequence affects, for example, the requirements for generation reserve.

Last, but not least, planners and operators have had decades of experience to assess the accuracy of – and get comfortable with – the clustering schemes in systems with hydropower. However, the insertion of renewables has not only been very fast but also changed significantly the operation pattern, leading to unexpected events such as "wind spills" in the hydro-dominated US Pacific Northwest system and to negative spot prices in Germany and other countries. For this reason, there is a great interest in representing much shorter intervals (and chronology) in SDDP's operating problem for each stage.

As seen above, there is no methodological difficulty in representing 730 hours per month in the operating problem; the major concern is the (also seen) very large impact of two orders of magnitude on execution time.

1.5 Proposed Methodology

In this work, we propose a methodology that allows for the accurate chronological representation of hourly (or sub-hourly) intervals in SDDP with a very modest increase in computational effort. As mentioned previously, the first basic idea is to represent the immediate cost function explicitly. In this case, the operating problem (1-1 - 1-10) would be represented as follows:

$$\alpha_t(\hat{v}_t) = Min\beta_t(e_t) + \alpha_{t+1} \tag{1-11}$$

$$v_{t+1,i} = \hat{v}_{t,i} + \hat{a}_{t,i} - (u_{t,i} + \nu_{t,i}) + \sum_{u \in U_i} (u_{t,u} + \nu_{t,u}), \forall i \in I \quad \leftarrow \pi^h_{t,i} \tag{1-12}$$

$$v_{t+1,i} \leq \overline{v}_i, \forall i \in I \tag{1-13}$$

$$u_{t,i} \leq \overline{u}_i, \forall i \in I \tag{1-14}$$

$$e_{t,i} = \rho_i u_{t,i}, \forall i \in I \tag{1-15}$$

$$\alpha_{t+1} \geq \sum_i \hat{\phi}^p_{t+1,i} \times v_{t+1,i} + \hat{\sigma}^p_{t+1}, \forall p \in P \quad \leftarrow \pi^{\alpha p}_{t,i} \tag{1-16}$$

It is interesting to observe that problem (1-11 - 1-16) no longer represents the time intervals $\tau = 1, \ldots, \mathcal{T}$ and, therefore, the load supply for each interval. All these equations and constraints are now represented by $\beta_t(e_t)$.

This means that, if $\beta_t(e_t)$ were available, SDDP's computational effort would, in principle, be the same for one average block; or hourly intervals; or five-minute intervals, which would be a significant computational advantage.

1.5.1 Equality of opportunity costs at the optimal solution

The above formulation also makes it easier to show the immediate and future water values, seen previously for the simple example of figure 1.1.1. The immediate water value of each hydro plant i is the multiplier $\pi^h_{t,i}$ associated to the water balance equations 1-12 at the optimal solution. In turn, the future water value is the coefficient $\hat{\phi}^p_{t+1,i}$ of the hyperplane p that is binding for constraint 1-16 at the optimal solution [2]. It is also possible to obtain the hydroelectric plant's opportunity costs, which are, as mentioned before, the result of the division of the water values by the hydroelectric plants' production factor.

[2] If more than one hyperplane is binding, we know from LP theory that the water value is a subgradient, i.e. a convex combination of the coefficients, where the weights are the multipliers $\pi^{\alpha p}_{t,i}$ associated to the hyperplane constraints.

It is interesting to observe that, if the hydroelectric plants do not hit turbine limits, i.e. do not turbine at all or turbine at its maximum capacity, in the solution of the operation problem, the opportunity costs of all hydro plants have spatially the same value at the optimal solution. We will use this fact in the proposed methodology. We present the proof of this statement in appendix C.

1.5.2 Representation of the ICF

As seen, the immediate cost function $\beta_t(e_t)$ represents the thermal operation cost required to meet the residual load, i.e., after the scheduled hydro e_t is used. We can see from the operation problem (1-1 - 1-10) that $\beta_t(e_t)$ can be formulated as the following LP:

$$\beta_t(e_t) = Min \sum_j c_j \sum_\tau g_{t,\tau,j} \tag{1-17}$$

$$\sum_\tau e_{t,\tau,i} = e_{t,i} \qquad \forall i \in I \tag{1-18}$$

$$e_{t,\tau,i} \leq \overline{e}_i \qquad \forall \tau \in \mathcal{T}, i \in I \tag{1-19}$$

$$\sum_i e_{t,\tau,i} + \sum_j g_{t,\tau,j} = \hat{\delta}_{t,\tau} \qquad \forall \tau \in \mathcal{T} \tag{1-20}$$

$$g_{t,\tau,j} \leq \overline{g}_j \qquad \forall \tau \in \mathcal{T}, j \in J \tag{1-21}$$

Because the function parameters $e_{t,i}$ are on the RHS of the constraints of an LP problem, we know from LP theory that $\beta_t(e_t)$ is a piecewise linear function. Therefore, it can be represented as:

$$\beta_t \geq \sum_i \hat{\mu}^l_{t,i} \times e_{t,i} + \hat{\Delta}^l_t, \forall l \in L \tag{1-22}$$

The constraints 1-22 will be used in our proposed formulation of the operation problem, presented next.

1.6 Operation problem with an analytical immediate cost function

The objective of this work is to replace the operation problem formulation (1-1 -1-10) by the following formulation:

$$\alpha_t(\hat{v}_t) = Min\ \beta_t + \alpha_{t+1} \tag{1-23}$$

$$v_{t+1,i} = \hat{v}_{t,i} + \hat{a}_{t,i} - u_{t,i} - \nu_{t,i} + \sum_{m \in U_i} (u_{t,m} + \nu_{t,m}) \qquad \forall i \in I \tag{1-24}$$

$$v_{t+1,i} \leq \overline{v}_i \qquad \forall i \in I \tag{1-25}$$

$$u_{t,i} \leq \overline{u}_i \qquad \forall i \in I \tag{1-26}$$

$$e_{t,i} = \rho_i u_{t,i} \qquad \forall i \in I \tag{1-27}$$

$$\alpha_{t+1} \geq \sum_i \hat{\phi}^p_{t+1,i} \times v_{t+1,i} + \hat{\sigma}^p_{t+1} \qquad \forall p \in P \tag{1-28}$$

$$\beta_t \geq \sum_i \hat{\mu}^l_{t,i} \times e_{t,i} + \hat{\Delta}^l_t \qquad \forall l \in L \tag{1-29}$$

Where the constraints 1-29 are pre-calculated. As discussed previously, this operation problem is much smaller than (1-1 - 1-10) and, therefore, can be solved more efficiently. In addition, the same effective relaxation techniques applied to the FCF constraints 1-28 can be applied to the ICF constraints 1-29, further increasing the efficiency.

1.7 Organization of the work

In chapter 2 we describe the calculation of $\beta_t(e_t)$ for a simpler case with just one hydro plant. We show that:

1. The number of segments in the piecewise linear function is J+1, where J is the number of thermal plants in the system;

2. It is only necessary to calculate $\beta_t(e_t)$ for *two values* to build the entire piecewise function, i.e. although the number of segments depends on the number of thermal plants, the computational effort does not depend on them;

3. It is not necessary to solve the thermal dispatch problem (1-17 - 1-21) to calculate $\beta_t(e_t)$; we show that the problem can be decomposed into $(J+1) \times \mathcal{T}$ comparisons of two pairs of numbers, which can be carried out in parallel.

As a consequence of features (1)-(3), the computational effort for pre-calculating $\beta_t(e_t)$ in this simpler case is negligible.

In chapter 3, we address the case of multiple hydro reservoirs. We show that, although in theory we would have to evaluate $\beta_t(e_t)$ for 2^I values, where I is the number of hydro plants, we can take advantage of the optimality

condition discussed above, that all hydroelectric opportunity cost values are equal at the optimal solution, to reduce the problem dimensionality, and, consequently, diminish the number of function evaluations, once more to just two. As a consequence, the computational effort of calculating $\beta_t(e_t)$ for the multi-reservoir case is also very small. Finally, we present the results we obtained when applying the methodology to the Panama country.

In chapter 4, we extend the proposed methodology to solve systems with multiple electrical areas, for example Brazil's four regions, or Central Americas' six-country regional pool. We show that the computational effort in this case is higher than the previous cases for two reasons: (i) the number of function evaluations is 2^R, where R is the number of regions; and (ii) It is no longer possible to decompose the thermal dispatch problem (1-17 - 1-21) into independent comparisons of two values.

Despite these limitations, we show that the computation effort of pre-calculating $\beta_t(e_t)$ can still be very small if we take advantage of the problem characteristics:

1. In the case of the higher number of function evaluations (2^R instead of 2), they can be carried out in parallel. As a consequence, the total time corresponds to that of one function evaluation;

2. In the case of multi-area systems, we show that the thermal dispatch problem (1-17 - 1-21) decomposes into J$\times\mathcal{T}$ separate max-flow problems, which again can be solved in parallel. Although the max-flow algorithms are more efficient than general LP solvers, we can further decrease the solution time by using the max flow – min cut theorem to transform the optimization problem into the verification of the max value of a set of linear constraints;

We finish this chapter by applying the proposed methodology to the Central America regional market, where we solve the operation problem for two interconnected countries (Panamá and Costa Rica) and three countries (the previous two plus Nicarágua). In all cases, the speedups were of two orders of magnitude, when compared with the solution of the standard operation problem (1-1 - 1-10).

Finally, Chapter 5 presents the conclusions and proposals for further research, in particular the representation of storage devices such as batteries in the calculation of the immediate cost function.

1.8 Survey of the literature

The need to consider uncertainties in capacity expansion problem on parameters such as fuel costs, equipment outages and demand resulted in the creation of a new type of model in the 1980's: probabilistic production costing (PPC). The basic idea is to obtain average operating costs of thermal systems by solving several operation minimization problems and varying the uncertain parameter. However, solving operation minimization problems can be very time consuming. There are several alternative algorithms proposed to solve this problem. (11) introduces a review on them. Many of them rely on the Baleriaux method ((4) and (9)).

Although much faster than solving optimization problems, this approach does not take into account time chronology. In other words, the Baleriaux method does not consider energy transference between stages, as each stage and scenario problem is solved independently. As a consequence, hydroelectric plants' representation needs to be simplified.

(20) proposed a modified algorithm that aimed to maintain chronology between stages (hydrothermal production costing). The algorithm was based on solving this type of problem as reliability problems, using the Baleriaux method and network flow representation.

Later, a different approach to solve HPC was proposed by (10). This work introduced the concept of the immediate cost function, that represents operative costs as function of the total hydroelectric generation in the stage. Furthermore, the idea that this function can be calculated by alternating the hydroelectric dispatch positions and using the Baleriaux method was also introduced by (10). Also, in order to limit the number of total calculations of the immediate cost function as they increase with the number of hydroelectric plants, (10) proposed to iteratively calculate it, using Dantiz-Wolfe decomposition (15).

In this work, we aim to solve hydrothermal operation problems with the help of the concepts presented above, using the immediate cost function in SDDP. Furthermore, we will propose a methodology that aims to calculate the immediate cost function previously to SDDP execution, instead of obtaining it by using decompositions methods.

1.9 Contributions of this work

The main contributions of this work are: (i) development of a new and computationally efficient methodology for multiscale representation (e.g.

hourly or sub-hourly for wind, weekly for hydro) of generation devices in each stage of stochastic operation problems; (ii) showing that the representation of convex functions by hyperplanes, originally restricted to the FCFs in SDDP, is a flexible modeling tool that, in addition, allows the use of efficient relaxation techniques - plus GPUs - in the problem solution; (iii) showing that the decomposition of probabilistic operation problems into easier-to-solve supply reliability problems, which were originally developed for a non-chronological "load block" framework, can be efficiently applied to deterministic chronological problems.

2
Analytical ICF for a one-hydro system

2.1
Problem formulation

For ease of presentation, we reproduce below the immediate cost problem (1-17 - 1-21), with only one hydro:

$$\beta_t(e_t) = Min \sum_j c_j \sum_\tau g_{t,\tau,j} \tag{2-1}$$

$$\sum_\tau e_{t,\tau} = e_t \tag{2-2}$$

$$e_{t,\tau} \leq \overline{e} \qquad \forall \tau \in \mathcal{T} \tag{2-3}$$

$$e_{t,\tau} + \sum_j g_{t,\tau,j} = \hat{\delta}_{\tau,t} \qquad \forall \tau \in \mathcal{T} \tag{2-4}$$

$$g_{t,\tau,j} \leq \overline{g}_j \qquad \forall \tau \in \mathcal{T}, j \in J \tag{2-5}$$

2.2
Example

We will illustrate the main concepts for a small system with one hydro plant and 3 thermal plants. The plant capacities and costs are shown in table 2.1.

	Thermal 1 (T1)	Thermal 2 (T2)	Thermal 3 (T3)	Hydro 1 (H)
Cost ($/MWh)	8	12	15	-
Capacity (MW)	10	5	20	10

Table 2.1: Small example data

The hydro plant production factor was assumed to be 1 MWh/m^3 . We also assume that the operation problem has only 3 hours. Table 2.2 shows the hourly residual loads (demand – renewable production).

Hour	Load (MWh)
1	24
2	31
3	11

Table 2.2: Load used in example

2.3 Approach 1: solve the operation problem for discrete values of hydroelectric generation

The most direct – and inefficient - approach is to discretize the monthly hydro production e_t into K values, $\hat{e}_t^k, k = 1, \ldots, K$, ranging from zero to the maximum hydro energy (hydro plant at full capacity for the entire month) and solve the operation problem (2-1 - 2-5) for each discrete value $\hat{e}_t^k$. For example, the optimization problem for the example above considering a total hydroelectric generation of 20 MWh for all hours would be presented as:

$$\begin{aligned}
\beta_t(20) = Min\ & 8g_{1,1} + 12g_{1,2} + 15g_{1,3} + \\
& 8g_{2,1} + 12g_{2,2} + 15g_{2,3} + 8g_{3,1} + 12g_{3,2} + 15g_{3,3} \\
& e_1 + e_2 + e_3 = 20 \\
& e_1, e_2, e_3 \leq 10 \\
& e_1 + g_{1,1} + g_{1,2} + g_{1,3} = 24 \\
& e_2 + g_{2,1} + g_{2,2} + g_{2,3} = 31 \\
& e_3 + g_{3,1} + g_{3,2} + g_{3,3} = 11 \\
& g_{1,1}, g_{2,1}, g_{3,1} \leq 10 \\
& g_{1,2}, g_{2,2}, g_{3,2} \leq 5 \\
& g_{1,3}, g_{2,3}, g_{3,3} \leq 20
\end{aligned}$$

The result for K = 100 (1% intervals) is shown in figure 2.1. The horizontal axis in the figure is the total hydro generation e_t (in MWh) and the vertical axis is immediate cost $\beta_t(e_t)$ (in $).

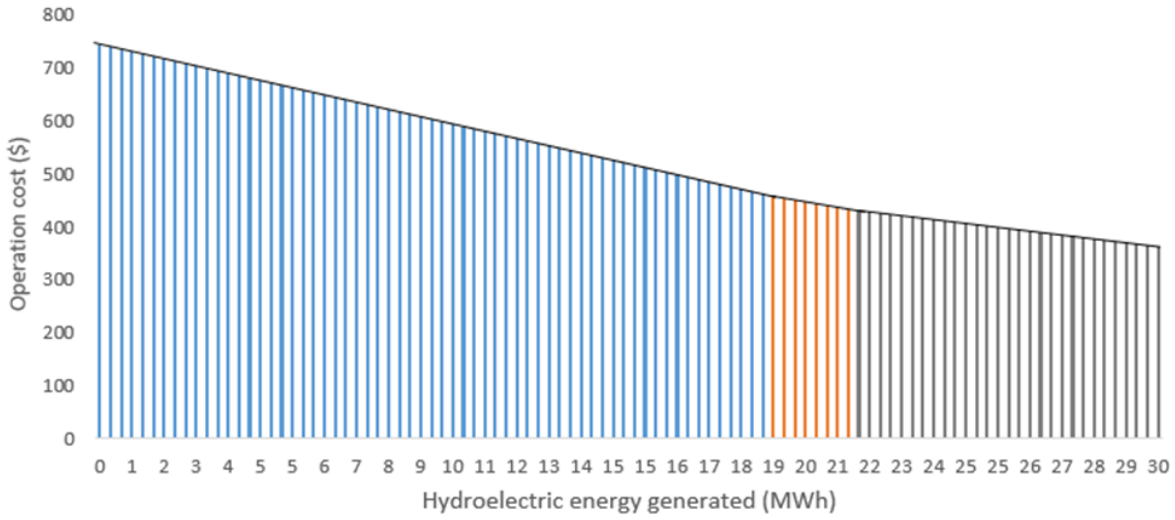

Figure 2.1: Immediate cost function of the example system

It is possible to see that the immediate cost function is piecewise linear, as mentioned in chapter 1. We will show that it is possible to take advantage on the problem structure in order to obtain the immediate cost function more efficiently.

2.3.1 Analytical representation of the immediate cost function

2.3.1.1 Convex combination

Because $\beta_t(e_t)$ is a piecewise linear function, it can be represented as a convex combination of the discrete values:

$$\begin{bmatrix} \beta_t \\ e_t \end{bmatrix} = \sum_k \mu_k \begin{bmatrix} \hat{\beta}_t^k \\ \hat{e}_t^k \end{bmatrix} \tag{2-6}$$

$$\sum_k \mu_k = 1 \tag{2-7}$$

2.3.1.2 Piecewise linear representation

A convex combination (figure 2.1) can always be transformed into a set of hyperplanes (figure 2.2), and vice-versa. Each hyperplane of a given stage t is represented as:

$$\beta_t^l = \hat{\mu}_t^l e_t^l + \hat{\Delta}_t^l, \forall l \in L \tag{2-8}$$

Angular and linear coefficients are calculated by:

$$\hat{\mu}_t^l = \frac{(\hat{\beta}^{l+1} - \hat{\beta}^l)}{\hat{e}^{l+1} - \hat{e}^l}, \forall l \in L \tag{2-9}$$

$$\hat{\Delta}_t^l = \hat{\beta}^l - \hat{\mu}_t^l \hat{e}^l, \forall l \in L \tag{2-10}$$

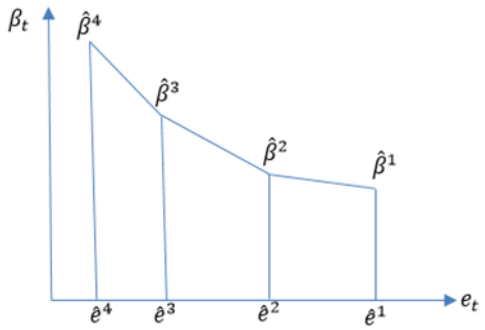

Figure 2.2: Immediate cost piecewise linear function

2.4 Approach 2: Lagrangian relaxation

The ICF curve 2-6 - 2-7 can be built much more efficiently if we take advantage of the problem structure. We see in figure 2.3 that there is only one *coupling constraint* in the problem (2-1 - 2-5) (constraint 2-2) , i.e. that has variables from different time intervals.

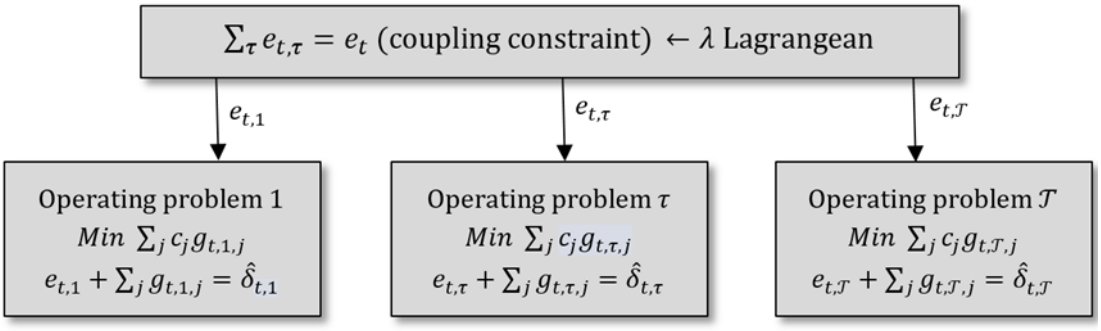

Figure 2.3: Hydroelectric energy generation problem structure

This means that if we take the Lagrangean of that constraint, $\lambda(\sum_\tau e_{t,\tau} - e_t)$, the problem can be decomposed into T separate optimization subproblems.

$$\beta_{t,\tau}(\lambda) = Min \sum_j c_j g_{t,\tau,j} + \lambda e_{t,\tau} \tag{2-11}$$

$$e_{t,\tau} + \sum_j g_{t,\tau,j} = \hat{\delta}^s_{\tau,t} \tag{2-12}$$

$$g_{t,\tau,j} \leq \overline{g}_j \qquad \forall j \in J \tag{2-13}$$

$$e_{t,\tau} \leq \overline{e} \tag{2-14}$$

Note that subproblem (2-11 - 2-14) can be interpreted as the optimal operation of a thermal system with J+1 generators, where the extra generator, with "operating cost" λ, is the hydro plant.

In the next sections, we will show that the combination of Lagrangian relaxation and other transformations allows the calculation of $\beta_t(e_t)$ with a very small computational effort. The algorithmic developments will be described in three steps:

1. The piecewise linear function $\beta_t(e_t)$ can be calculated by solving J+1 Lagrange operation problems, corresponding to the function breakpoints.

2. Each Lagrange operation problem can be decomposed into supply reliability subproblems, which can be solved with simple arithmetic operations.

3. This decomposition also allows the calculation of $\beta_t(e_t)$ from the solution of only two Lagrange problems, instead of J+1.

2.4.1 Calculation of the immediate cost function from the solution of Lagrange operation problems

Suppose, without loss of generality, that the thermal plants are ordered by increasing operating costs $c_j, \forall j = 1, \ldots, J$. If we examine the Lagrangian problem (2-11 - 2-14), it is easy to see that there are only J+1 *different optimal solutions*, corresponding to the following ranges of values for the Lagrange multiplier:

(1) $\lambda < c_1$ $\leftarrow$ hydro is the first to be dispatched
(2) $c_1 < \lambda < c_2$ $\leftarrow$ hydro is dispatched after the first (cheapest) thermal generator
(3) $c_1 < \lambda < c_2$ $\leftarrow$ hydro is dispatched after the second thermal generator
$\vdots$
(J+1) $c_J < \lambda$ $\leftarrow$ hydro is dispatched after all thermal generators.

It is also interesting to observe that the exact value of λ in each range does not matter for the construction of $\beta_t(e_t)$; only the position of the hydro plant on the loading order of the generators is relevant.

As a consequence, we can construct $\beta_t(e_t)$ by solving (J+1) operating problems for each time interval $\tau = 1, \ldots, \mathcal{T}$. The procedure is implemented as shown in 1

Algorithm 1 Calculation of the immediate cost function from the solution of Lagrange operation problems

1: **for** each hydro position in the loading order $k = 1, \ldots, J+1$ **do**
2: Let $\hat{\lambda}^k$ = any value in the range (k) above.
3:
4: **for** each interval $\tau = 1, \ldots, \mathcal{T}$ **do**
5:
6: Solve the operation subproblem $\beta_{t,\tau}(\hat{\lambda}^k)$ and calculate:

- The total thermal cost $\hat{\beta}^k_{t,\tau} = \sum_j c_j \hat{g}^k_{t,\tau,j}$ ($\hat{}$optimal solution).
- The optimal hydro generation $\hat{e}^k_{t,\tau}$

7: **end for**
8: Calculate the total thermal cost and hydro generation for the stage t:

- $\hat{\beta}^k = \sum_\tau \hat{\beta}^k_{t,\tau}$
- $\hat{e}^k_t = \sum_\tau \hat{e}^k_{t,\tau}$

9: **end for**

For instance, for $\lambda = 7$, we would obtain the immediate cost and hydroelectric generation of hour 1 for the example problem by solving the problem below:

$$\beta_{t,1}(7) = Min\ 8g_1 + 12g_2 + 15g_3 + 7e \tag{2-15}$$
$$e + g_1 + g_2 + g_3 = 24 \tag{2-16}$$
$$g_1 \leq 10 \tag{2-17}$$
$$g_2 \leq 5 \tag{2-18}$$
$$g_3 \leq 20 \tag{2-19}$$
$$e \leq 10 \tag{2-20}$$

This problem was solved with the aid of a commercial optimization package. The optimal solution is presented in table 2.4

Obj Func	$\hat{\beta}^k_{t,1}$	e	g_1	g_2	g_3
572.36	362.36	30	20.92	9	5.8

Table 2.3: Optimal dispatch for the example optimization problem

Where $\hat{\beta}^k_{t,1} = 8\hat{g}_1 + 12\hat{g}_2 + 15\hat{g}_3$.

As in the previous case, $\beta_t(e_t)$ can be represented as a convex combination of the discretized pairs [operating cost $\hat{\beta}^k_t$; hydro generation $\hat{e}^k_t$] resulting from the above procedure or, equivalently, as the set of hyperplanes used in our proposed formulation.

2.4.2 Decomposition of the immediate cost function into supply reliability subproblems

Suppose the following thermal dispatch problem where, as assumed above, the generators are ordered by increasing operation cost.

$$Min\ z = \sum_j c_j g_j \tag{2-21}$$

$$\sum_j g_j = \hat{\delta} \tag{2-22}$$

$$g_j \leq \overline{g}_j \qquad \forall j \in J \tag{2-23}$$

It is well known from the probabilistic production costing literature that the least-cost operation problem (2-21 - 2-23) can be solved as a set of reliability evaluation sub-problems:

1. Define $\delta_0 = \hat{\delta}$

2. Let δ_j represent the energy not supplied when the cheapest j generators are loaded at their maximum capacity:

$$\delta_j = Max(d - \overline{G}_j, 0), \forall j \in J \tag{2-24}$$

Where $\overline{G}_j = \sum_{k=1}^{j} \overline{g}_k$

3. It is easy to see that the power produced by each generator j at the optimal solution of the thermal dispatch problem (2-21 - 2-23), represented as g^*_j, is given by the decrease in unserved energy after the generator is loaded:

$$g^*_j = \delta_{j-1} - \delta_j, \forall j \in J \tag{2-25}$$

4. Finally, the optimal operation cost is given by:

$$z^* = \sum_j c_j g_j^* \tag{2-26}$$

Let us consider the thermal generators and system load of the example system. The optimization model for this example would be as shown in equations (2-27 - 2-31).

$$Min\ z = 8g_1 + 12g_2 + 15g_3 \tag{2-27}$$
$$g_1 + g_2 + g_3 = 24 \tag{2-28}$$
$$g_1 \leq 10 \tag{2-29}$$
$$g_2 \leq 5 \tag{2-30}$$
$$g_3 \leq 20 \tag{2-31}$$

This problem was solved with the aid of a commercial optimization package. The optimal solution is presented in table 2.4

Obj Func	g_1	g_2	g_3
275	10	5	9

Table 2.4: Optimal dispatch for the example optimization problem

Using the approach mentioned above, we will calculate the optimal thermal dispatch for hour 1 of the example as follows:

1. $\delta_0 = 24$

2. We start dispatching the cheapest generator (T1) and update δ: δ_1 = Max (24 - 10 ,0) = 14.
   Then we move to the second cheapest thermal plant (T2):
   δ_2 = Max (24 - 15 ,0) = 9.
   Finally, we obtain δ_3:
   δ_3 = Max (24 - 35 ,0) = 0.

3. Now, we calculate the generation of each thermal plant:
   g_1^* = 24 - 14 = 10 MWh
   g_2^* = 14 - 9 = 5 MWh
   g_3^* = 9 - 0 = 9 MWh

4. Finally, we obtain the optimal operation cost:
   $10(MWh) \times 8(\$/MWh) + 5(MWh) \times 12(\$/MWh) + 9(MWh) \times 15(\$/MWh) = 275\$$

In summary, steps 1-4 above allow us to solve a thermal dispatch with simple arithmetic operations which, additionally, can be carried out in parallel.

2.4.3 Calculation of the immediate cost function from the solution of supply reliability problems

Because the Lagrangian problem (2-11 - 2-14) is equivalent to a thermal dispatch problem, the above methodology can be applied directly to the calculation of $\beta_t(e_t)$:

Algorithm 2 Calculation of the immediate cost function from the solution of supply reliability problems

for each hydro position in the loading order $k = 1, \ldots, J+1$ **do**
Let $\hat{\lambda}^k$ = any value in the range (k) above.

for each interval $\tau = 1, \ldots, \mathcal{T}$ **do**

Solve the operation subproblem $\beta_{t,\tau}(\hat{\lambda}^k)$ using the reliability decomposition scheme (1)-(4) above and calculate the total thermal cost as:

$$\hat{\beta}^k_{t,\tau} = \sum_{j \neq k} c_j \hat{g}^k_{t,\tau,j} \tag{2-32}$$

Note that the k^{th} generator was excluded from the summation 2-32 because it corresponds to the hydro plant. The optimal hydro generation is:

$$\hat{e}^k_{t,\tau} = \hat{g}^k_{t,\tau,j} \tag{2-33}$$

end for
Calculate the total thermal cost and hydro generation for the stage t:

- $\hat{\beta}^k = \sum_\tau \hat{\beta}^k_{t,\tau}$
- $\hat{e}^k_t = \sum_\tau \hat{e}^k_{t,\tau}$

end for

As in the previous case, $\beta_t(e_t)$ is represented as a convex combination of the the discretized pairs [operating cost $\hat{\beta}^k_t$; hydro generation $\hat{e}^k_t$]:

$$\begin{bmatrix} \beta_t \\ e_t \end{bmatrix} = \sum_k \mu_k \begin{bmatrix} \hat{\beta}^k_t \\ \hat{e}^k_t \end{bmatrix}$$

Below, we present the calculation of the immediate cost points given λ in different ranges:

$\lambda = 7$

Hour	Obj Func	$\beta_{t,\tau}(\hat{\lambda}^k)$	e	g_1	g_2	g_3
1	198	128	10	10	4	0
2	297	277	10	10	5	5.8
3	77.36	7.36	10	0.92	0	0
total	572.36	362.36	30	20.92	9	5.8

Table 2.5: Optimal dispatch ($\lambda = 7$)

Which is exactly the same solution we found by solving the optimization problem (table 2.4)

$\lambda = 10$

Hour	Obj Func	$\beta_{t,\tau}(\hat{\lambda}^k)$	e	g_1	g_2	g_3
1	198	128	10	10	4	0
2	297	227	10	10	5	5.8
3	86.44	80	0.92	10	0	0
total	581.44	435	20.92	30	9	5.8

Table 2.6: Optimal dispatch ($\lambda = 10$)

$\lambda = 13$

Hour	Obj Func	$\beta_{t,\tau}(\hat{\lambda}^k)$	e	g_1	g_2	g_3
1	203	140	9	10	5	0
2	297	227	10	10	5	5.8
3	91.04	91.04	0	10	0.92	0
total	591.04	458.04	19	30	10.92	5.8

Table 2.7: Optimal dispatch ($\lambda = 13$)

$\lambda = 20$

Hour	Obj Func	$\beta_{t,\tau}(\hat{\lambda}^k)$	e	g_1	g_2	g_3
1	275	275	0	10	5	9
2	377	377	0	10	5	15.8
3	91.04	91.04	0	10	0.92	0
total	743.04	743.04	0	30	10.92	24.8

Table 2.8: Optimal dispatch ($\lambda = 20$)

$\beta_t(e_t)$ can be calculated by evaluating only two positions of the hydro plant in the loading order, first ($k = 1$) and last ($k = J + 1$)

Next, we show how to obtain the intermediate points of the immediate cost function.

2.4.4 Calculation of intermediate points of the immediate cost function from the two extreme points

Let $\hat{g}^k_{t,j}$ and $\hat{e}^k_t$ represent respectively the energy produced by each thermal generator j and by the hydro plant in stage t:

- $\hat{g}^k_{t,j} = \sum_\tau \hat{g}^k_{t,\tau,j}, \forall t \in T, j \in J$
- $\hat{e}^k_t = \sum_\tau \hat{e}^k_{t,\tau}, \forall t \in T$

Suppose now that we want to solve the operating problem for the case with the hydro plant in position k = 3, i.e. it is dispatched after thermal plants 1 and 2. We already have calculated the optimal dispatch, presented in table 2.7.

We now show how the problem solution $\hat{g}^3_{t,j}$ and $\hat{e}^3_t$ can be obtained from the solutions for k = 1 (hydro first) and k = J+1 (hydro last):

1. For thermal plants 1 and 2 (loaded *before* the hydro in this example), results come from the case where hydro is loaded last (k = J+1)

$$\begin{bmatrix} \hat{g}^3_{t,1} & = & \hat{g}^{J+1}_{t,1} \\ \hat{g}^3_{t,2} & = & \hat{g}^{J+1}_{t,2} \end{bmatrix} \tag{2-34}$$

   By looking at table 2.8, we see that the generation of thermal plants 1 and 2 for the first hour should be 10 MWh and 5 MWh respectively. If we compare to the results of table 2.7, we see that in fact the generations are the same.

2. For thermal plants 3 to J (loaded after the hydro), results come from the case where hydro is loaded first (k = 1)

$$\begin{bmatrix} \hat{g}^3_{t,3} & = & \hat{g}^1_{t,3} \\ \dots & & \\ \hat{g}^3_{t,J} & = & \hat{g}^1_{t,J} \end{bmatrix} \tag{2-35}$$

In other words, if we compare the generations of thermal plant 3 in both tables 2.5 and 2.7 we see that they are the same, 0 MWh.

3. Finally, the hydro generation is obtained subtracting the total thermal generation from the load:

$$\hat{e}^3_t = d_t - \sum_j \hat{g}^3_{t,j} \tag{2-36}$$

The total hydroelectric generation should be 24 - 10 - 5 - 0 = 9 MWh. This is the same value found in table 2.7

The reason for expression 2-34 is that the generation of a given plant does not depend on the loading of the plants that come afterwards. In other words, the generation of thermal plants 1 and 2 is the same for the case where the hydro is loaded in position 3; or in position 4; and so on, until the last position, J+1, which is the one we had calculated.

In turn, expression 2-35 can be understood by looking at equation 2-25: the generation of a given plant is given by the difference between the unserved energy for the total generation capacity loaded before and after that plant is included. For our example, this means that the generation of thermal plant 3 is the same for the loading orders $H : T_1 : T_2$ (which we have calculated); $T_1 : H : T_2$; and $T_1 : T_2 : H$

Finally, total cost of dispatches which the hydroelectric plant is in an intermediate position can be obtained as previously shown.

As in the previous cases, $\beta_t(e_t)$ can be represented as a convex combination of the discretized pairs [operating cost $\hat{\beta}^k_t$; hydro generation $\hat{e}^k_t$] resulting from the above procedure or, equivalently, as the set of hyperplanes used in our proposed formulation.

2.5 Extracting hourly results from the analytical ICF

Once the optimal solution of the one-stage operation problem using the analytical ICF has been obtained, it is possible to extract the hourly production of each plant, if desired.

The reason is that, as seen in section 2.4.4, the calculation of $\beta_t(e_t)$ for each position of the hydro in the loading order requires the energy produced by each thermal plant in each time interval (otherwise, we would not be able to calculate the total thermal operating cost). If this preprocessing information is stored, the hourly operation of each plant at the optimal solution can be obtained as a weighted combination of the hourly values for each segment of $\beta_t(e_t)$ that is binding at the optimal solution.

For example, suppose that the optimal values of the convex weights are λ_3^* (hydro is in the third position in the loading order) $= 0.7$ and $\lambda_4^* = 0.3$ (remember that $\sum \lambda^* = 1$). The optimal generation of each thermal plant j (plus the hydro, which as seen is represented as an additional "thermal" plant) in the time interval τ, $g^*_{t,\tau,j}$, will be:

$$g^*_{t,\tau,j} = 0.7 \times \hat{g}^{k(=3)}_{t,\tau,j} + 0.3 \times \hat{g}^{k(=4)}_{t,\tau,j}$$

Where $\hat{g}^k_{t,\tau,j}$ is the (precalculated) generation of thermal plant j when the hydro is in the k^{th} position in the loading order.

3
Multiple hydro plant systems

For ease of presentation, we reproduce below the one-stage operation problem with multiple hydro plants and analytical ICF (1-23 -1-29):

$$\alpha_t(\hat{v}_t) = Min\ \beta_t + \alpha_{t+1} \tag{3-1}$$

$$v_{t+1,i} = \hat{v}_{t,i} + \hat{a}_{t,i} - u_{t,i} - \nu_{t,i} + \sum_{m \in U_i} (u_{t,m} + \nu_{t,m}) \qquad \forall i \in I \tag{3-2}$$

$$v_{t+1,i} \leq \overline{v}_i \qquad \forall i \in I \tag{3-3}$$

$$u_{t,i} \leq \overline{u}_i \qquad \forall i \in I \tag{3-4}$$

$$e_{t,i} = \rho_i u_{t,i} \qquad \forall i \in I \tag{3-5}$$

$$\alpha_{t+1} \geq \sum_i \hat{\phi}^p_{t+1,i} \times v_{t+1,i} + \hat{\sigma}^p_{t+1} \qquad \forall p \in P \tag{3-6}$$

$$\beta_t \geq \sum_i \hat{\mu}^l_{t,i} \times e_{t,i} + \hat{\Delta}^l_t \qquad \forall l \in L \tag{3-7}$$

Because we are dealing with multiple hydroelectric plants problems, the ICF is now a multivariate piecewise linear function, $\beta_t(e_{t,1}, \ldots, e_{t,i}, \ldots, e_{t,I})$. In theory, the extension of the ICF methodology from one hydro plant to I hydro plants is straigthforward: calculate the operating costs assuming that each hydro is a dummy thermal plant which is first (and last) in the loading order. Note, however, that we now have 2^I combinations of loading positions: all hydro first; $I-1$ hydro plants first and one of them last; $I-2$ hydro first and two of them last; and so on.

One approach to reduce the computational effort due to the number of combinations is to build $\beta_t(e_t)$ iteratively, using decomposition techniques ((10) and (8)).

In this work, we propose to reduce computational effort based on the optimality conditions of hydrothermal operation, mentioned previously: if the hydro plants do not reach turbining limits within the stage, all hydro opportunity costs at the optimal solution will be equal. In terms of the ICF calculation, the optimality condition means that all hydro plants will be at the same point in the loading order. In this case, the multivariate function $\beta_t(e_{t,1}, \ldots, e_{t,i}, \ldots, e_{t,I})$ can be replaced by a scalar function of the total hydro

generation, $\beta_t(\sum_i e_{t,i})$, as shown below.

$$\alpha_t(\hat{v}_t) = Min\ \beta_t + \alpha_{t+1} \tag{3-8}$$

$$v_{t+1,i} = \hat{v}_{t,i} + \hat{a}_{t,i} - u_{t,i} - \nu_{t,i} + \sum_{m \in U_i} (u_{t,m} + \nu_{t,m}) \qquad \forall i \in I \tag{3-9}$$

$$v_{t+1,i} \leq \overline{v}_i \qquad \forall i \in I \tag{3-10}$$

$$u_{t,i} \leq \overline{u}_i \qquad \forall i \in I \tag{3-11}$$

$$e_t = \sum_i \rho_i u_{t,i} \tag{3-12}$$

$$\beta_t \geq \hat{\mu}_t^l \times e_t + \hat{\Delta}_t^l \qquad \forall l \in L \tag{3-13}$$

$$\alpha_{t+1} \geq \sum_i \hat{\phi}_{t+1,i}^p \times v_{t+1,i} + \hat{\delta}_{t+1}^p \qquad \forall p \in P \tag{3-14}$$

Note that the hydro plants in water balance equations 3-9 and the FCF 3-14 are still represented individually (multivariate functions); the aggregation only applies to the ICF calculation. It is easy to see that the ICF calculation procedure for problem (3-8 - 3-14) is very similar to the case with a single reservoir. Next, we illustrate the application of the proposed analytical ICF technique to the operation of Panama, which is part of Central America's Regional Electricity Market (MER, in Spanish).

3.1 Case Study

The Central America's Regional Electricity Market (MER) is currently composed of six countries: Panama, Costa Rica, Nicaragua, Honduras, El Salvador and Guatemala. There is also an interconnection between Guatemala and Mexico, and plans for an interconnection between Panama and Colombia.

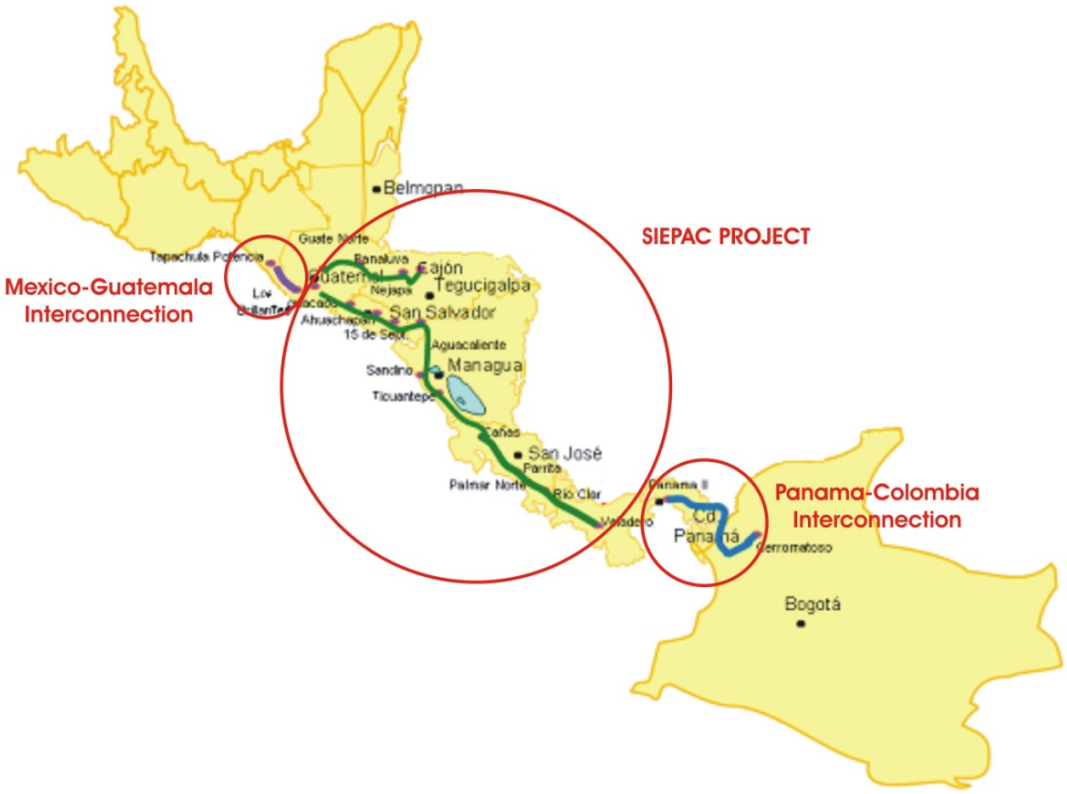

Figure 3.1: Central America's Regional Electricity Market (MER)

Figure 3.2 shows the main characteristics of each country (installed capacity and generation mix). We see that there is a wide mix of generation technologies, with a historically strong hydro share and, more recently, a fast insertion of wind, solar and biomass. The MER countries have used SDDP for both operation and expansion planning, and with the entrance of renewables, there is a great interest in having a stochastic policy calculation with hourly resolution.

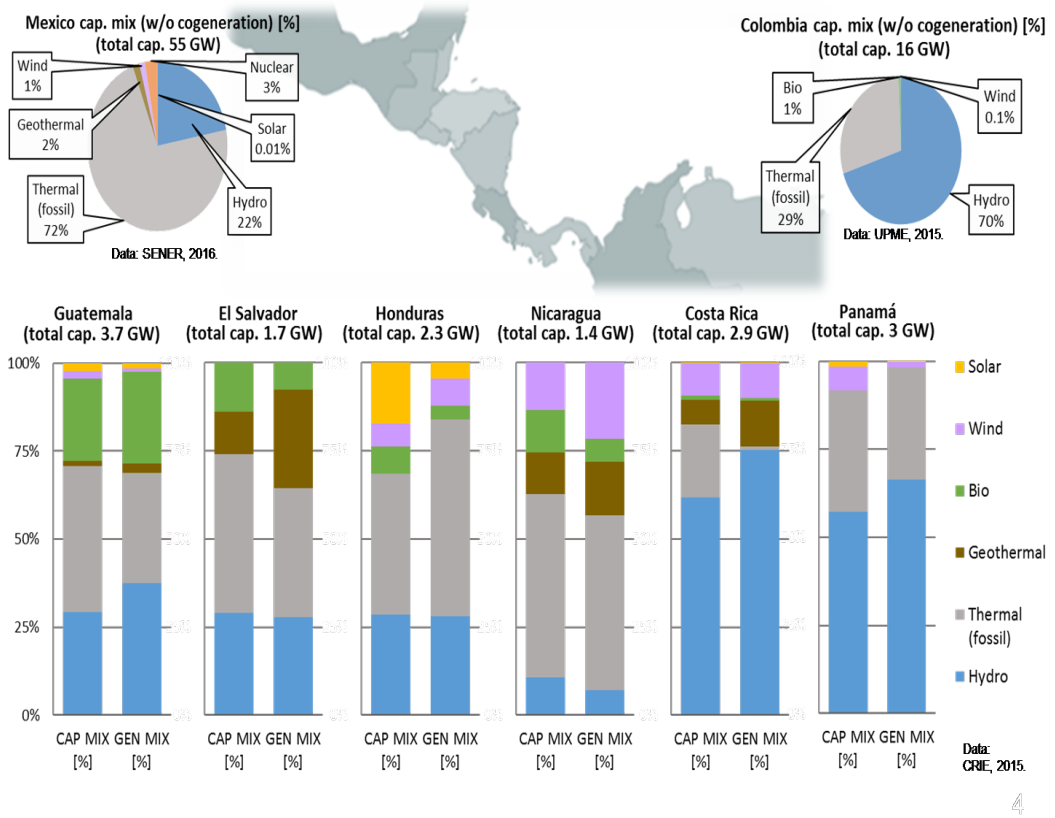

Figure 3.2: Central America, Mexico and Colombia: installed capacity and generation mix

We will illustrate the ICF calculation methodology for Panama and, in the next chapter, we will carry out multi-country studies taking into account the interconnection limits.

3.1.1 Panama

Figure 3.3 shows the main components of Panama's power system.

Figure 3.3: Panama's power system. Source: (14)

The Panama system has 42 hydro plants, 22 thermal plants and wind/solar renewable generation.

Figure 3.4 shows the loading curve (operating cost and cumulative capacity) of Panama's thermal plants.

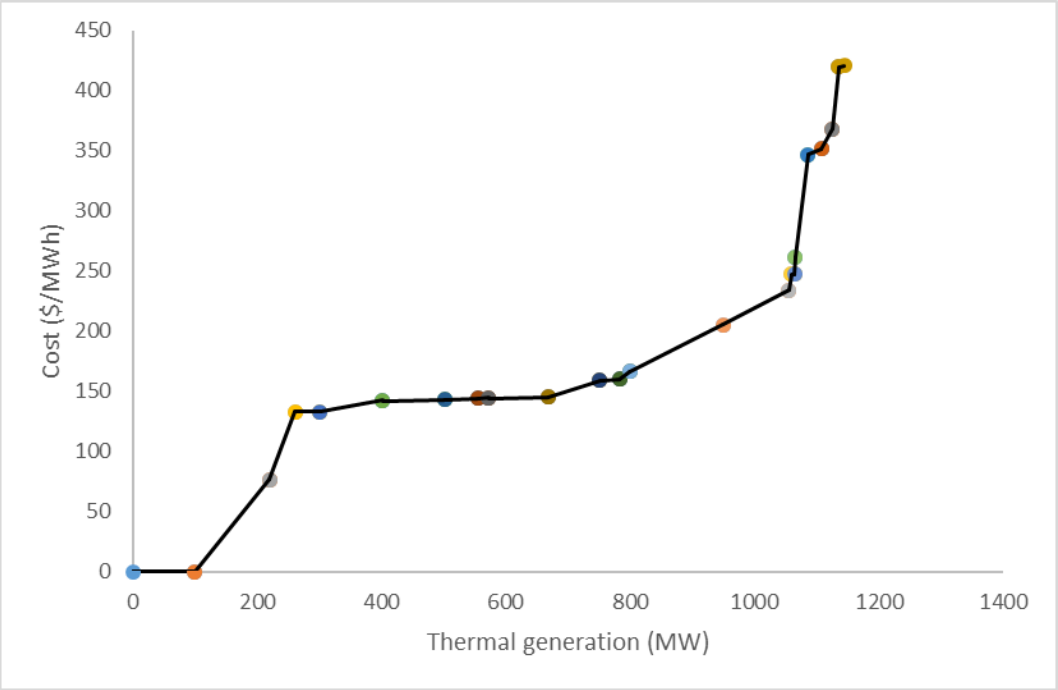

Figure 3.4: Panama's thermal plants: operating cost and cumulative installed capacity in March/2016

The figure 3.5 illustrate Panama's hourly load (month of March/2016).

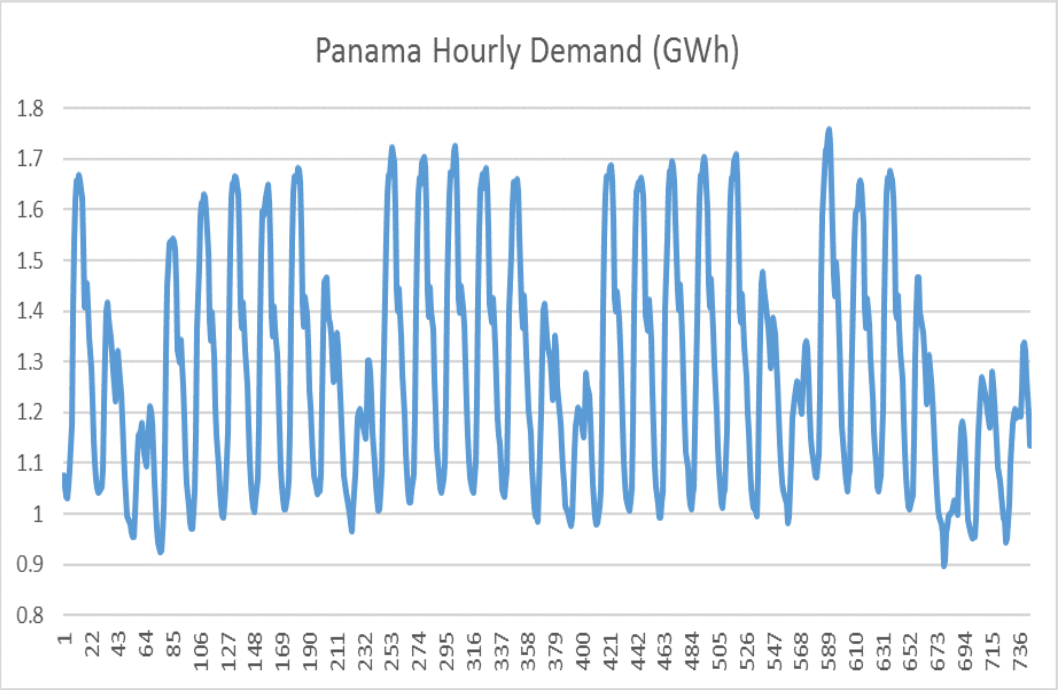

Figure 3.5: Panama hourly demand March/2016

3.1.2 Study description

The ICF calculation methodology was implemented in PSR's SDDP model (26), which is the official operations and planning software for the MER. We calculated the stochastic operation policy twice: (i) standard SDDP with hourly resolution (730 power balances in the one-stage operation problem); and (ii) SDDP with the ICF scheme. Figure 3.6 shows the analytical ICF for the month of March/2016 and one renewable scenario. As seen previously, the number of breakpoints is J (number of thermal plants, 22 in Panama's case) + 1 (the aggregated hydro generation).

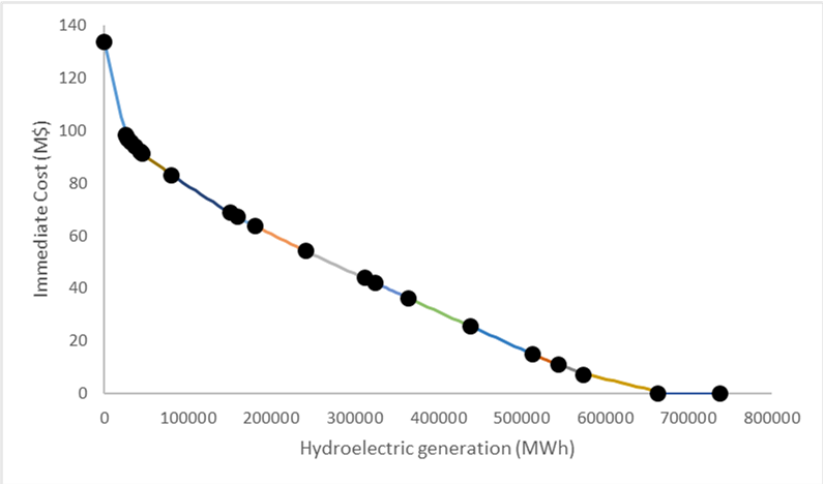

Figure 3.6: Panama case study: Analytical ICF for March/2016

The study horizon was two years (24 months), with 100 scenarios (inflows and renewable generation) in SDDP's forward simulation step and 30 conditioned scenarios ("openings") in the backward recursion step.

3.1.3 Computational results

The studies were run on an Amazon Cloud server with 32 processes. Convergence was achieved in 8 iterations. As seen previously, this means that the total number of one-stage problems solved was 8 (number of iterations) $\times$ 100 (number of scenarios in the forward simulation) $\times$ 31 (number of backward "openings" + 1) $\times$ 24 (number of stages) $\simeq$ 600 thousand. Total execution time with a standard hourly representation was 14 minutes; with the ICF, 3 seconds. This corresponds to a speedup of 287 times.

3.1.4 Accuracy of the ICF approximation

As seen previously, the ICF calculation effort was reduced with the assumption that all hydro plants have the same opportunity costs at the optimal solution of each one-stage operation problem. The accuracy of this assumption was verified by comparing the present value of the operation cost for each of the 100 scenarios in the final probabilistic simulation (after convergence has been achieved) of the ICF representation with the results of the standard SDDP model (hourly power balances in each stage). Figure 3.7 shows these present values in increasing order.

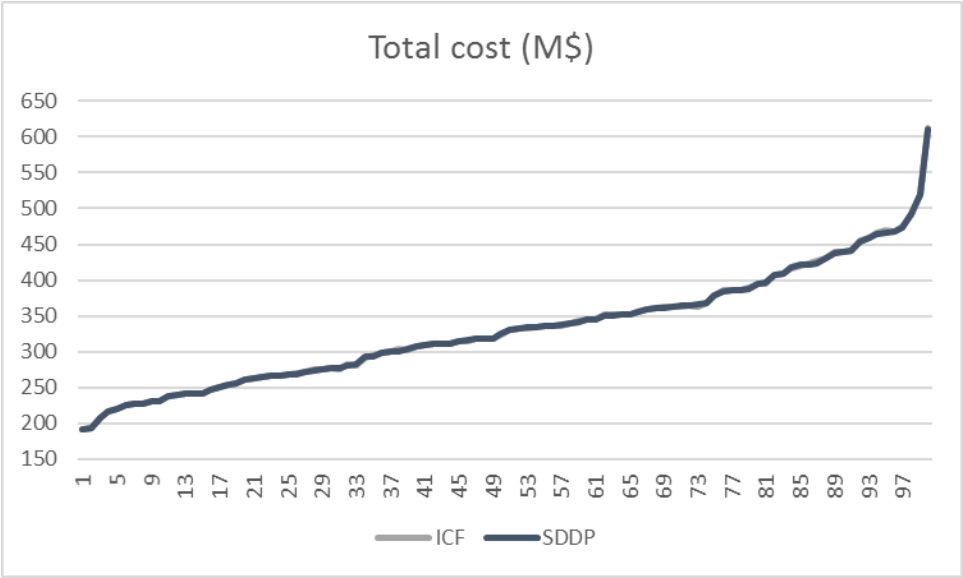

Figure 3.7: Present value of total operation cost along the study period (24 months)

The average cost difference was 0.01%, indicating that in this case the ICF represents very accurately the system operation.

In the next chapter, we extend the ICF methodology for multiple regions with power interchange limits.

4
ICF calculation algorithm for multi-area systems

In this section, we address the ICF calculation for systems with multiple electrical areas, such as Brazil's four regions (South, Southeast, North and Northeast) and Central America's six-country MER regional pool.

4.1
Multi-area operation problem

In the multi-area representation, the ICF $\beta_t(e_t)$ is extended to represent the power flow constraints between areas in the hourly power balance. As a consequence, the multi-area operation problem is very similar to the single-area problem of chapter 3. The only difference is that the hydro generation is now aggregated for each area r (equation 4-5).

$$\alpha_t(\hat{v}_t) = Min\ \beta_t(e_t) + \alpha_{t+1} \tag{4-1}$$

$$v_{t+1,i} = \hat{v}_{t,i} + \hat{a}_{t,i} - u_{t,i} - \nu_{t,i} + \sum_{m \in U_i} (u_{t,m} + \nu_{t,m}) \qquad \forall i \in I \tag{4-2}$$

$$v_{t+1,i} \leq \overline{v}_i \qquad \forall i \in I \tag{4-3}$$

$$u_{t,i} \leq \overline{u}_i \qquad \forall i \in I \tag{4-4}$$

$$e_{t,r} = \sum_{i \in \Omega_r} \rho_i u_{t,i} \qquad r \in R \tag{4-5}$$

$$\alpha_{t+1} \geq \sum_i \hat{\phi}^p_{t+1,i} \times v_{t+1,i} + \hat{\sigma}^p_{t+1} \ \leftarrow \pi^{\alpha p}_{t,i} \qquad \forall p \in P \tag{4-6}$$

Where
$r = 1, \ldots, R$ indexes electrical areas
Ω_r set of hydro plants in area r.

4.2
Multi-area ICF

In the multi-area case, $\beta_t(e_t)$ is a multivariate function of the hydro generation in each area, $\{e_{t,r},\ r = 1, \ldots, R\}$. The ICF problem is formulated as:

$$\beta_t(e_t) = Min \sum_{\tau} \sum_{j} c_j g_{t,\tau,j} \tag{4-7}$$

$$\sum_{\tau} e_{t,\tau,r} = e_{t,r} \qquad \forall r \in R \tag{4-8}$$

$$e_{t,\tau,r} \leq \overline{e}_r \qquad \forall \tau \in \mathcal{T}, r \in R \tag{4-9}$$

$$e_{t,\tau,r} + \sum_{j \in \Theta_r} g_{t,\tau,j} + \sum_{q \neq r} (f_{t,\tau}^{q,r} - f_{t,\tau}^{r,q}) = \hat{\delta}_{t,\tau}^{r} \qquad \forall \tau \in \mathcal{T}, r \in R \tag{4-10}$$

$$g_{t,\tau,j} \leq \overline{g}_j \qquad \forall \tau \in \mathcal{T}, j \in J \tag{4-11}$$

$$f_{t,\tau}^{q,r} \leq \overline{f}^{q,r} \qquad \forall \tau \in \mathcal{T} \tag{4-12}$$

$$f_{t,\tau}^{r,q} \leq \overline{f}^{r,q} \qquad \forall \tau \in \mathcal{T} \tag{4-13}$$

Where:

$\hat{\delta}_{t,\tau}^{r}$ residual load (demand – renewables) of area r

$f_{t,\tau}^{q,r}$ power flow from area q to area r

$\overline{f}^{q,r}$ maximum flow from area q to area r

Θ_r set of thermal plants in area r.

We see that (4-7 - 4-13) is a linear programming problem in which, again, $e_{t,r}$ appears only on the right hand side. As a consequence, $\beta_t(e_t)$ is a multivariate piecewise linear function of the hydro generation in each area:

$$\beta_t \geq \sum_{r} \hat{\mu}_{t,r}^{l} \times e_{t,r} + \hat{\Delta}_t^l, \forall l \in L \tag{4-14}$$

We now show how to pre-calculate the hyperplanes of expression 4-14

4.3 Disaggregation of the ICF problem into hourly subproblems

We see that the multi-area ICF (4-7 - 4-13) has the same structure as the single area problem, i.e. the only coupling constraints are those of equation 4-8 (disaggregation of the hydro generation for the stage, $e_{t,r}$, into hourly values $e_{t,\tau,r}$). Therefore, we can apply the same Lagrangian scheme used for the single-area problem to decompose the problem into T separate hourly multi-area operation subproblems.

Also similarly to the single-area scheme, the hydro generation in each hourly subproblem is represented as a thermal plant whose "operating cost" and, thus, its position in the loading order, is given by the value of the Lagrange multiplier associated with constraint 4-8.

4.4

Solving the hourly subproblem for the extreme hydro positions

In the previous chapter, we showed that, although the ICF function had J linear segments, it could be calculated by solving the operation problem only twice: (i) with hydro first in the loading order; and (ii) with hydro last. The operating costs of intermediate loading positions (hydro second; third etc.) are then calculated as combinations of solutions (i) and (ii).

In the multi-area problem, the same logic applies. However, the number of hydro loading positions is now 2^R: hydro of all regions first; all hydro last; hydro of $R-1$ regions first, the other last; and son on. We show in the next sections that the computational effort of solving these problems can be substantially reduced if we apply concepts from *network flow* theory. Initially, we show that the hourly subproblem is a min-cost network flow.

4.5 Example

We will apply the main concepts of this chapter using another small

•

example. Let us represent two areas: A and B. Area A is the one represented in chapter 2. Interconnection capacity from area A to area B is 15 MW and from area B to A is 20 MW. Let us assume that area B has a generation capacity of 35 MW, provided by one thermal plant (T4) with cost of 10 $/MWh and a residual (demand – renewable production) hourly load specified in table 4.1.

Hour	Load (H)
1	30
2	20
3	24

Table 4.1: Load used in example for area B

4.6 The hourly subproblems are min-cost network flows

Given a set of Lagrange multipliers λ_t^r, the operating subproblem of hour τ of stage t is:

$$Min \sum_{j} c_j g_{t,\tau,j} + \sum_{r} \lambda_t^r e_{t,\tau,r} \tag{4-15}$$

$$e_{t,\tau,r} \leq \overline{e}_r \qquad \forall r \in R \tag{4-16}$$

$$e_{t,\tau,r} + \sum_{j \in \Theta_r} g_{t,\tau,j} + \sum_{q \neq r} (f_{t,\tau}^{q,r} - f_{t,\tau}^{r,q}) = \hat{\sigma}_{t,\tau}^{r} \qquad \forall r \in R \tag{4-17}$$

$$g_{t,\tau,j} \leq \overline{g}_j \qquad \forall \tau \in \mathcal{T}, j \in J \tag{4-18}$$

$$f_{t,\tau}^{q,r} \leq \overline{f}^{q,r} \tag{4-19}$$

$$f_{t,\tau}^{r,q} \leq \overline{f}^{r,q} \tag{4-20}$$

The hourly problem (4-15 - 4-20) is a special type of linear programming, known as minimum cost network flow.

For the first hour of the example, the network flow optimization problem (for $\lambda^1 = 7$)is represented as:

$$\begin{aligned} Min\ 8g_1 + 12g_2 + 15g_3 + 10g_4 + 7e_1 \\ e_1 \leq 10 \\ e_1 + g_1 + g_2 + g_3 + (f^{2,1} - f^{1,2}) = 24 \\ g_4 + (f^{1,2} - f^{2,1}) = 30 \\ g_1 \leq 10 \\ g_2 \leq 5 \\ g_3 \leq 20 \\ g_4 \leq 35 \\ f^{1,2} \leq 15 \\ f^{2,1} \leq 20 \end{aligned}$$

Next, we show that min-cost network flow problem can be decomposed into $J + R$ *multi-area reliability evaluation problems*, similarly to the developments of chapter 3.

4.7 Solving min cost problems by max flows in a network

The same problem presented in the next section can also be represented as a graph, as shown in figure 4.1

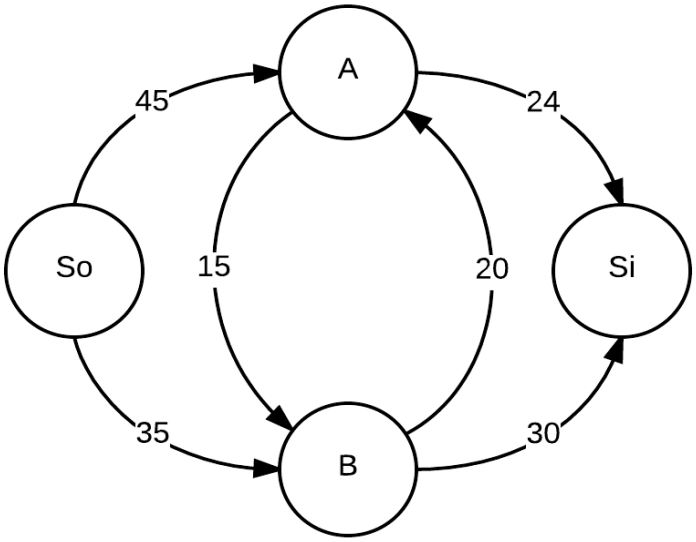

Figure 4.1: Resulting graph for example

Now, in order to find the dispatch we need to find the maximum flow that can be transferred from node So (Source) to node Si (Sink). As it can be seen from figure 4.1 it is very intuitive to consider that the maximum flow between those nodes cannot exceed the capacities of the arcs So->A and So->B, which are the generation capacities of each area, once there are no other arcs from where energy could flow from node So. Also, the maximum flow cannot exceed the capacities of arcs A->Si and B->Si, which represent the demand of each area. Finally, it is clear that the flow between areas cannot exceed the network capacity and also needs to be taken into account (arcs A->B and B->A).

Finding the maximum flow of the network, however, does not mean finding the least cost dispatch. Taking advantage on the special structure of our problem, however, we can iteratively add generators (increasing So->A and So->B arcs' capacities) to the graph following merit dispatch order and solve the maximum flow problem. By doing this, we would be able to obtain the optimal dispatch and costs.

4.8 Solving max-flow problems by min cuts

Formally, we can obtain the maximum flow from a graph by solving an optimization problem that aims to maximize the flow between nodes So and Si subject to arcs' capacities. It is also proved (22) that the optimal flow optimization problem is strongly related to the cut minimization problem. One of the greatest advantages of finding the minimum cut in the graph instead

of calculating its maximum flow is that, in small problems, cuts can be easily enumerated.

A cut is characterized by the minimum set or arcs that isolate node So from node Si. That is, if we were to remove those arcs, there would be no flow from node So to node Si. In this example, there are four cuts. The first two cuts are quite obvious: cut 1 is composed by arcs {So->A,So->B} and cut 2 by arcs {A->Si,B->Si}. The last two are less obvious: cut 3 is composed by arcs {So->A,B->A,B->Si} lastly, cut 4 is composed by arcs So->B,A->B,A->Si. All cuts are demonstrated graphically in figure 4.2.

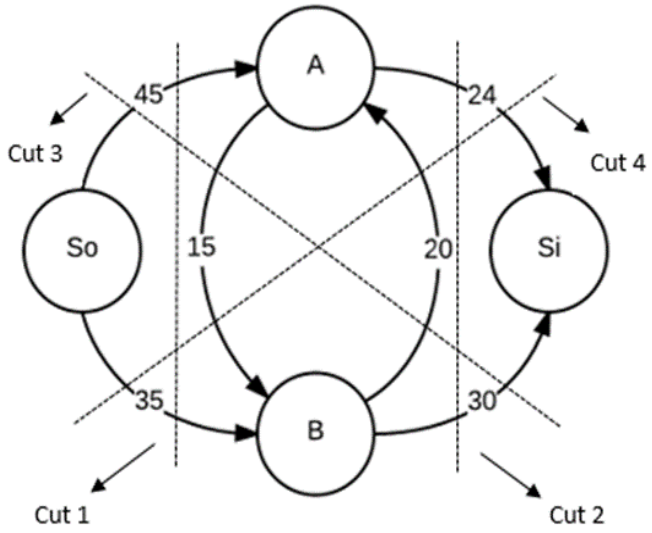

Figure 4.2: Example graph's cuts

Finally, we show that the max-flow problems can be solved more efficiently as the direct calculation of the maximum value of a set of linear constraints, similar to the FCF and ICF hyperplanes of the operation problem. This is achieved through the application of the max flow-min cut theorem, described next. Table 4.2 shows the cuts' values for this example.

CUT	Value (MW)
1	80
2	54
3	95
4	74

Table 4.2: Example graph cut values

The minimum cut value for this example would therefore be of 54 MW. As shown, instead of solving the maximum flow optimization problem, we can simply enumerate all cuts in the graph and find the minimum cut. With the concepts of the previous sections, we finally arrived at the proposed solution algorithm for the calculation of $\beta_t(e_t)$, presented in the following section.

4.9 Proposed algorithm

Algorithm 3 Calculation of the immediate cost function using Min-Cut approach

```
Set initial graph with generation capacity arcs with capacity equal to zero and obtain graph's cuts
for every combination of first/last loading order positions for the regional hydro generation do
    for every hour do
        for every generator in dispatch order do
            Add the cheapest possible generator, set resulting graph
            Obtain graph's minimum cut
            The current plant generation will be obtained by subtracting the previous minimum cut value of the current minimum cut value
        end for
        Calculate total dispatch cost
    end for
    Aggregate generation values and cost for all stage hours
end for
Obtain the remaining dispatches using the previously calculated dispatches
```

Now let us apply the algorithm to our small system. We already exemplified the cuts in this graph, as shown in figure 4.2. As there is only one region that has a hydroelectric plant (area A), we only need to perform calculations twice, considering the hydroelectric in first and last in the dispatch. Considering it to be in the first position, for the first hour, we would need to perform the following calculations:

1. Add the hydroelectric plant to the graph and obtain its minimum cut:

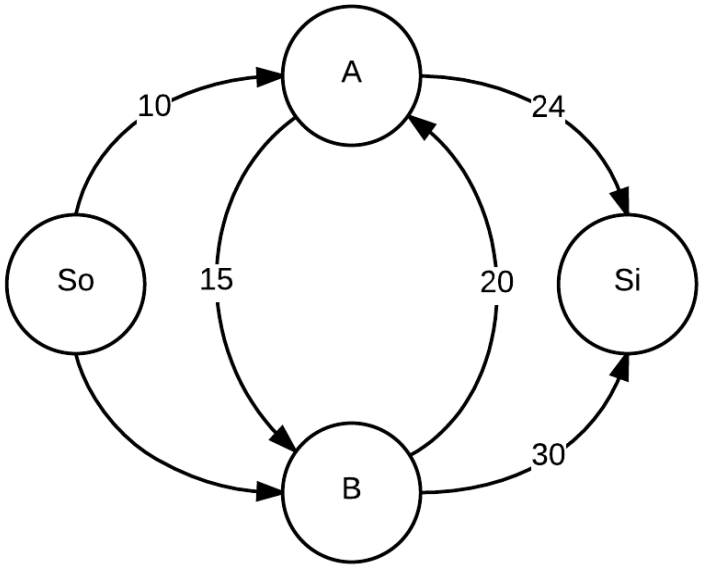

Figure 4.3: Resulting graph for example step 1

The minimum cut So->A, So->B in this case is 10. As this is the first generator, its total generation is exactly the minimum cut value: 10 MW.

2. Add the cheapest thermal plant (T1) to the graph and obtain its minimum cut:

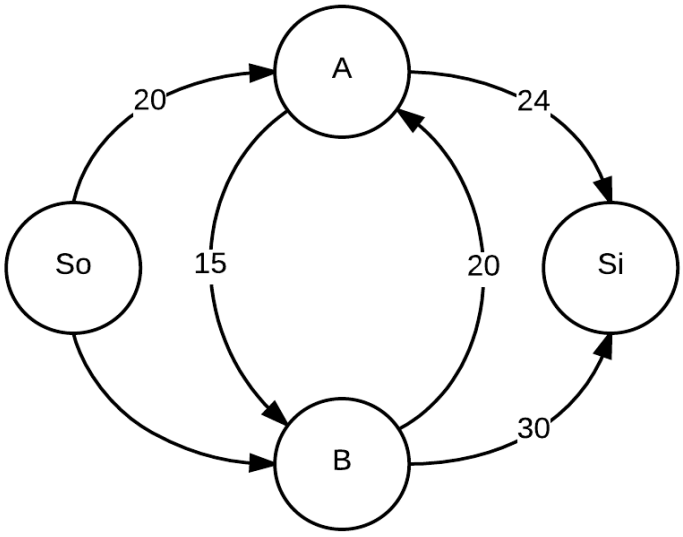

Figure 4.4: Resulting graph for example step 2

The minimum cut So->A, So->B in this case is 20. The total generation of thermal plant T1 is, therefore is 20 - 10 = 10 MWh.

3. Add the second cheapest thermal plant (T4) to the graph and obtain its minimum cut:

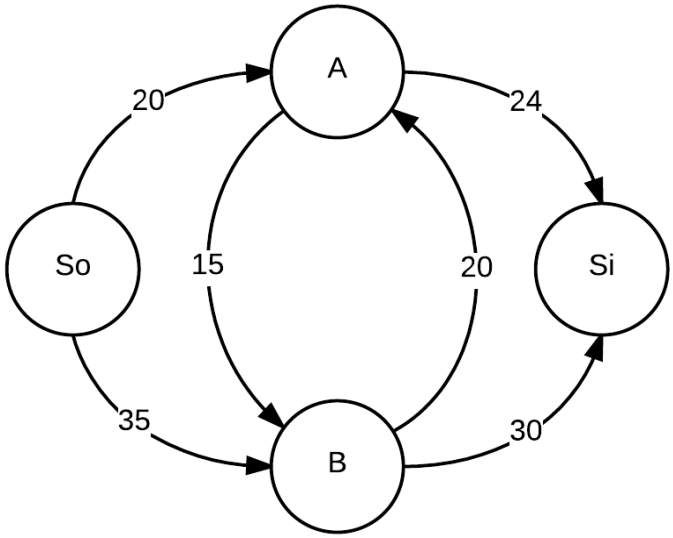

Figure 4.5: Resulting graph for example step 3

The minimum cut A->Si, B->Si in this case is 54. The total generation of thermal plant T4 is, therefore is 54 - 20 = 34 MWh.

4. As the total generation is equal to the demand of both areas, we know that the generation of all other thermal plants is zero. The total dispatch cost for hour 1 is: $10(MWh) \times 8(\$/MWh) + 34(MWh) \times 10(\$/MWh) = 420$ \$

After performing this calculation for every single stage hour, we then aggregate the values of all hours to obtain ICF points.

4.10 Creating ICF hyperplanes

As seen in the previous chapters, the algorithm above produces "vertices", i.e. vectors of total operation cost and hydro generation that correspond to "breakpoints" of the piecewise linear function. The ICF is then represented as a convex combination of those vertices:

$$\begin{bmatrix} \beta_t \\ e_{t,j} \\ \dots \\ e_{t,j} \end{bmatrix} = \sum_l \lambda_l \begin{bmatrix} \hat{\beta}_t^l \\ \hat{e}_t^{1l} \\ \dots \\ \hat{e}_t^{\mathrm{Rl}} \end{bmatrix} \tag{4-21}$$

The next, and final step, of the proposed scheme is to move from the "vertex" to the "hyperplane" representation of equation 4-14. In the single region case, as seen in section 2.3.1.2, the transformation is geometrically obvious, and straightforward. For the multivariate case, however, there is no direct conversion scheme. We then applied a convex hull generation algorithm, described next.

4.11 Transformation of vertices into hyperplanes using convex hulls

The Qhull project (29) implementation relies on Quickhull algorithm (5) and has achieved high reliability and performance and have actually been used by MATLAB and Python's SciPy (28) as default convex hull generators. There are several other convex hull algorithms, such as(13), (1) and (2).(3) performs an evaluation on the efficiency of several convex hull algorithms.

In this work, we used Python's Qhull library (28) to perform the conversion between vertex representation and hyperplane representation. Figure 4.6 shows an example of immediate cost plan set for a case with 2 electrical areas.

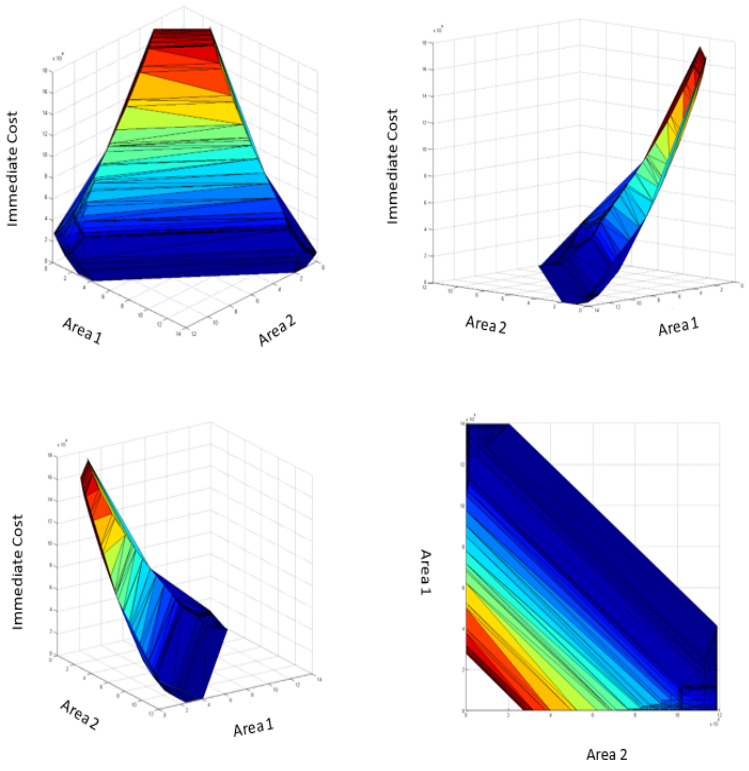

Figure 4.6: 2 Area example of immediate cost function. Horizontal axis represent total hydroelectric generation of each area and vertical axis represents total immediate costs.

(21) proposes an upper bound limit to the number of hyperplanes that will be created given the number of vertices (equation 4-22).

$$f_d = \binom{n - \left\lfloor \frac{d+1}{2} \right\rfloor}{n-d} + \binom{n - \left\lfloor \frac{d+2}{2} \right\rfloor}{n-d} \tag{4-22}$$

Where:

n is the number of vertices

d is the number of dimensions of the vertices

After transforming the points into hyperplanes, we can use the same algorithm used to reduce the number of future cost cuts inserted in the problem. That is, as mentioned before, we can solve the problem iteratively inserting new cuts as they are violated in the previous iterations.

4.12 Case studies

After the immediate cost plans are finally calculated, we need to insert them in the optimization model. In this chapter, we will discuss the results obtained by using the immediate cost approach in SDDP in multi-area real cases.

The algorithm used to calculate the immediate cost function was programmed in Fortran 77 and the calculation time was irrelevant. Even though, once this algorithm can be implemented in GPUs, the processing time of the immediate cost function in Fortran 77 is not relevant to this work. In the next sections, we will present 2 study cases. The first one comprehends the effects of using the immediate cost function in a 2-area system: Panama and Costa Rica. The second, consists in evaluating its performance on a 3 area system (Panama, Costa Rica and Nicaragua).

All simulations performed were 2 years long (monthly stages), including the years of 2015 and 2016. Also, 100 inflow scenarios (forwards) were considered.

We will compare optimal costs obtained in SDDP run of an hourly problem equations(1-1 - 1-10) and a problem using the ICF hyperplanes equations(3-8 - 3-14). Cut relaxation was used for both FCF and ICF cuts. Finally, we will present a comparison between computational times. Simulations were performed on a computer with the following configuration: 60GB of RAM memory, 32 cores and frequency of 2.8 GHz. SDDP runs were performed in parallel, using 7 processors.

4.13
Panama and Costa Rica system

Costa Rica area has 36 hydroelectric plants and 12 thermal plants. As there are in total 34 thermal plants and 2 areas, the total number of possible hydroelectric dispatch combinations is 1,225. Using the upper bound formula presented before (equation 4-22), there would be, at maximum, a total of 2,446 hyperplanes to be considered in the model. As we eliminated redundant planes, for this specific case, around 600 hyperplanes were considered.

A cost comparison between the ICF and hourly problems can be seen in figure 4.7.

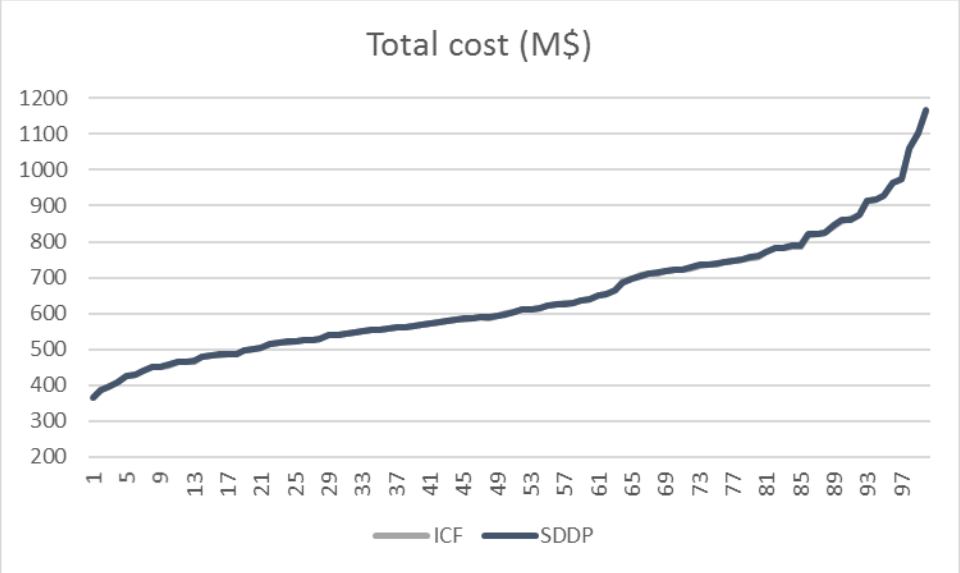

Figure 4.7: Comparison of total costs per scenario between hourly and ICF representation for Panama and Costa Rica system

The average percentage of cost difference between both resolutions was 0.05%. The total time speed up of the ICF solution when compared to the hourly representation was of 317 times.

4.14
Panama, Costa Rica and Nicaragua system

Nicaragua area has 5 hydroelectric plants and 26 thermal plants. In total, there are 60 thermal plants in the system and a total of 226,981 different hydroelectric dispatch position combinations. Using the upper bound formula presented before (equation 4-22), there would be, at maximum, in the order of 10^{10}, hyperplanes to be considered in the model. However, for this special

case, only 20,000 hyperplanes were created. Total costs per scenario from both hourly and ICF executions are shown in figure 4.8.

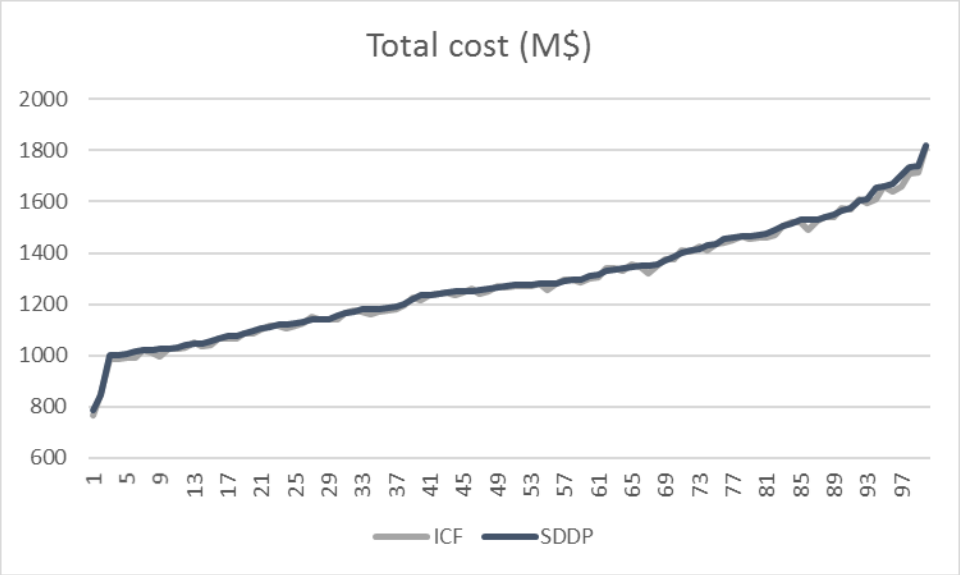

Figure 4.8: Comparison of total costs per scenario between hourly and ICF problem for Panama, Costa Rica and Nicaragua system

The average percentage of cost difference between both resolutions was 0.61%. The total time speed up of the ICF solution when compared to the hourly representation was of 434 times.

4.15 Time Comparison

From the previous sections, it was possible to see that the immediate cost function approach resulted in very similar optimal costs when compared to the hourly model. In this section we will compare computational times of both approaches.

In figure 4.9, we see the total speedup when comparing the hourly model with the ICF model in all cases. In average, the ICF approach is 346 times faster than the hourly representation.

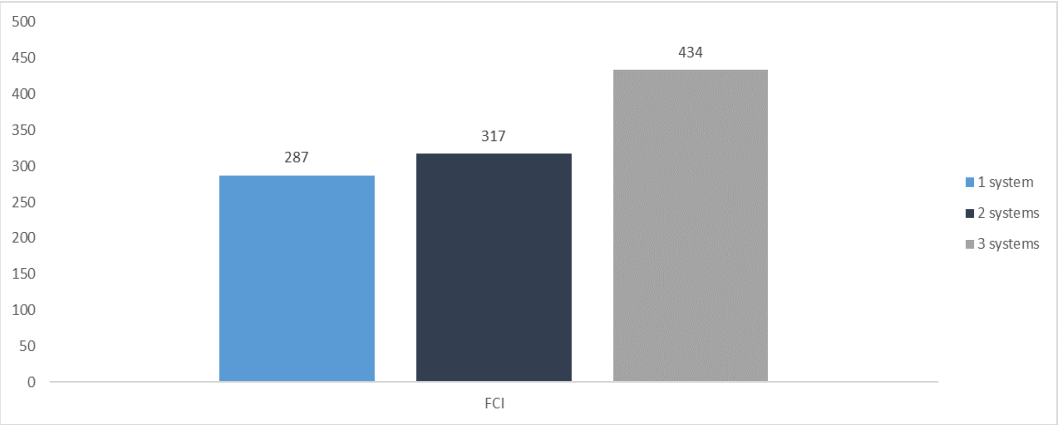

Figure 4.9: Total speedup of the ICF problem for all cases

5
Conclusions and future work

5.1
Conclusion

With the penetration of renewable energy sources in the energy market, there has been an increase in the uncertainty of energy generation in small time frames. Renewable generation sources such as solar and wind power present volatile generation during the day. The representation of such variations is crucial, especially to countries without hydroelectric power, which is capable to adjust to these fluctuations almost immediately. In this scenario, hourly (or sub-hourly) representation in operation problems became very important.

In this work, we demonstrated that using the immediate cost function is much faster than solving the hourly problem and yet, it is capable of reproducing the latter optimal costs. We also presented an algorithm to obtain this function previously to the execution of the optimization itself. As the algorithm can be performed in parallel and using GPUs, executing it should little time.

The immediate cost function has several applications when solving operation problems. In SDDP, it enables hourly resolution during policy phase, which may be computationally intractable when using hourly representation variables depending on the size of the problem. In addition to that, it is also possible to represent batteries when using this approach, which will be crucial to handle renewable source energy generation intermittence.

5.2
Future work

5.2.1
Run-of-river hydroelectric plants and batteries

Many possible future implementations are compatible with the ideas presented in this work. First, even in the hour disaggregation model, we did not use hourly water balance constraints. That is because the hydroelectric plants considered in this work are able to regulate themselves within the stage period, which is, in this work, a month.

Obviously, it is not always the case. Many hydroelectric plants have small reservoirs and, therefore, are not capable of regulating themselves, even for a whole week. Fortunately, there is still a way to consider this type of regulatory constraints implicitly in the immediate cost function. Let us consider a single area system 3-hour operation problem. As mentioned before, such problem can be represented as a minimum cut graph problem. In the previous approach, we would find the minimum graph cut for each hour, in order to obtain the immediate cost function. However, in this case, the system has exactly one hydroelectric plant that has little regulatory capacity. It is intuitive that, if there is a plant with some regulatory capacity between hours, then hourly graphs would be somehow connected, as energy can be passed from one hour to another. An example of the resulting graph is given in figure 5.1.

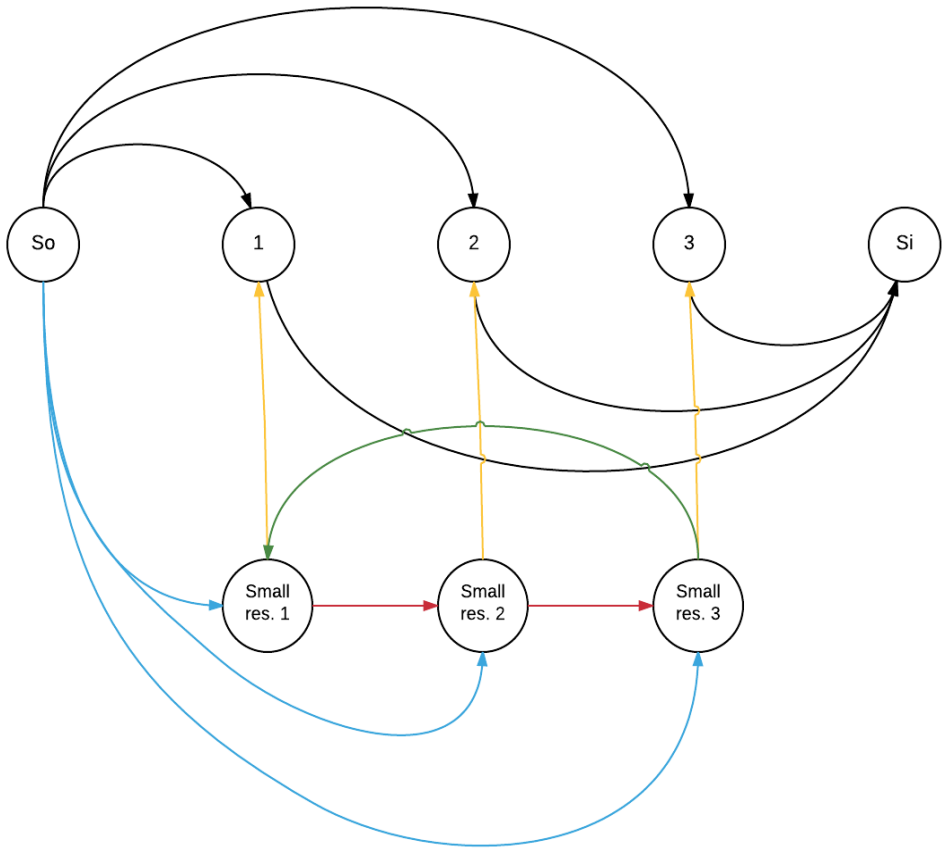

Figure 5.1: Resulting system graph when representing hydroelectric plants with little regulation capacity

In figure 5.1 black arcs represent capacity and demand arcs, explained previously. Lower nodes, called "Small res.", represent the hydroelectric plant with small regulation capacity in each hour. Blue arcs represent the amount

of inflow energy of the hydroelectric plant in each hour and red arcs represent the maximum stored energy (volume) that can flow from one hour to another. Yellow arcs represent the maximum generation of the hydroelectric and lastly, green arc assures that initial energy volume has to be equal to the final stage volume.

In addition to that, using the same approach proposed for hydro plants that have little regulation information, it is also possible to model batteries. The result for one single battery is shown in figure 5.2.

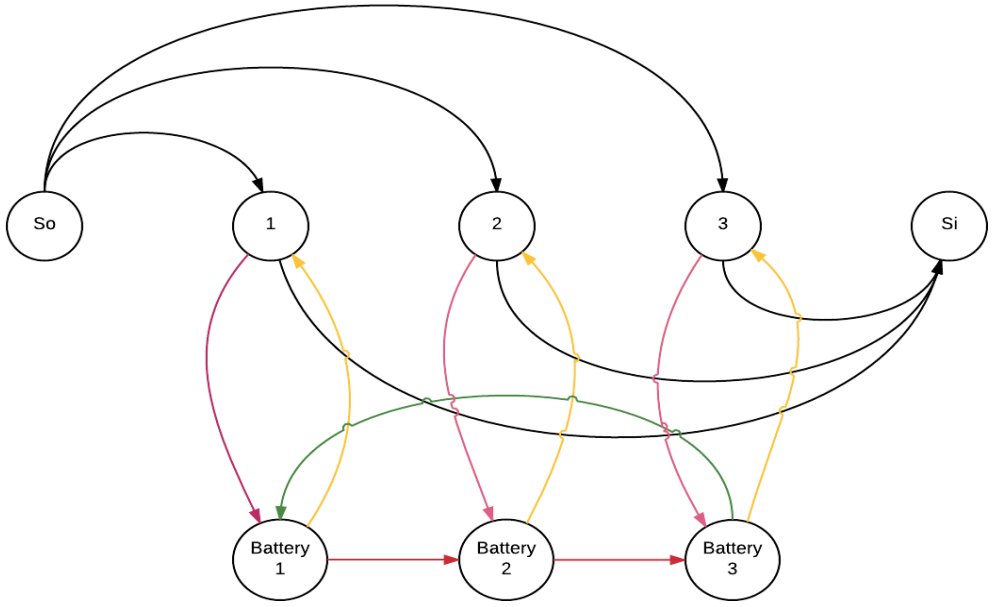

Figure 5.2: Resulting system graph when representing batteries

Note that there are two basic differences when comparing figure 5.1 with figure 5.2. First, there are no blue arcs in this graph. As batteries are only capable of storing previously generated energy, the only way it can receive energy is from the system itself. This leads to the second difference: there are new arcs (presented in pink) that transfer energy from the system to the battery. They represent the maximum energy that can be transferred to the battery in an hour. Red arcs still represent maximum storage and yellow arcs represent maximum energy transferring from the battery to the system.

5.2.2 Multiple scenario representation

As we expressed at the beginning of this work, hourly operation representation becomes necessary because of renewable generations variability. We

have shown that we can represent hourly operation using the immediate cost function but we did not show how we would represent renewable generation variability. As SDDP has several forward scenarios (see appendix B), it would be possible to pre-calculate the ICF for each renewable energy scenario and use them separately for each forward scenario. Another option would be as follows:

Let us assume that we want to represent S possible renewable generation scenarios. We already know how to calculate the immediate cost points for each scenario. We calculate the immediate cost points of all L hydroelectric dispatch positions using the residual demand. That is, for each scenario, we would have different residual demands to begin with. After the calculation, we would obtain the immediate cost points for every scenario (s) and every hydroelectric dispatch position (l):

$$\begin{bmatrix} \beta_s^l \\ e_s^l \end{bmatrix} \tag{5-1}$$

Now, we assemble the immediate cost points so that we have, in the same vector, points from every scenario calculated with the hydroelectric plant in the same dispatch position:

$$\begin{bmatrix} e_1^1 \\ e_2^1 \\ \vdots \\ e_S^1 \end{bmatrix} \begin{bmatrix} e_1^2 \\ e_2^2 \\ \vdots \\ e_S^2 \end{bmatrix} \cdots \begin{bmatrix} e_1^L \\ e_2^L \\ \vdots \\ e_S^L \end{bmatrix} \tag{5-2}$$

Each vector would have a correspondent β^l, which would be the average of the β_s^l of all s scenarios:

$$\overline{\beta}^l = \frac{\sum_s \beta_s^l}{S} \tag{5-3}$$

The resulting operation optimization problem would be as shown below:

$$\alpha_t(\hat{v}_t) = \min_{\lambda} \overline{\beta} + \frac{1}{S}\sum_{s} \alpha^s_{t+1}(v^s_{t+1}) \tag{5-4}$$

$$\overline{\beta} = \lambda_1\overline{\beta}^1 + \lambda_2\overline{\beta}^2 \ldots + \lambda_L\overline{\beta}^L \tag{5-5}$$

$$\begin{bmatrix} e^1 \\ e^2 \\ \vdots \\ e^S \end{bmatrix} = \lambda_1 \begin{bmatrix} e^1_1 \\ e^1_2 \\ \vdots \\ e^1_S \end{bmatrix} + \lambda_2 \begin{bmatrix} e^2_1 \\ e^2_2 \\ \vdots \\ e^2_S \end{bmatrix} + \ldots. + \lambda_L \begin{bmatrix} e^L_1 \\ e^L_2 \\ \vdots \\ e^L_S \end{bmatrix} \tag{5-6}$$

$$v^s_{t+1} = \hat{v}_t + a^s_t - \frac{e^s_t}{\rho} - w^s_t, \forall s \in S \tag{5-7}$$

$$v^s_{t+1} \leq \overline{v}, \forall s \in S \tag{5-8}$$

$$\frac{e^s_t}{\rho} \leq \overline{u}, \forall s \in S \tag{5-9}$$

$$\sum_{l} \lambda_l = 1 \tag{5-10}$$

$$\alpha^s_{t+1} \geq \hat{a}^p_{t+1} v^s_{t+1} + \hat{b}^p_{t+1}, \forall p \in P, s \in S \tag{5-11}$$

Where $\hat{v}_t$ is randomly sampled from the previous stage $t-1$ scenarios' final volumes (v^s_t).

As it can be seen in the model above, our only optimization variables are the λ. In other words, we are in fact choosing the hydroelectric plant's optimal dispatch position instead of optimal generation. Even further, we have different energy generations for every scenario s (e^s) as, depending on the amount of renewable generated energy, clearly the hydroelectric plant would generate more or less, regardless of its dispatch position.

Finally, it is clear that this scenario approach can be extended for several other different possible sources of variability, such as demand and inflows. As mentioned before, we calculate the immediate cost considering hydroelectric plants with little storage capacity. As state previously, arcs connecting the source node to the hydroelectric plant (blue arc shown in figure 5.1) represent the amount of inflow energy of the plant. As inflows are also uncertain, we can use this approach to represent its variability.

5.2.3
Obtaining hourly results and marginal costs

5.2.3.1
Obtaining hourly generation variables and costs

As it was seen in this work, the optimization problem that uses the immediate cost function does not have hourly variables. If we wish to obtain them,

we need to somehow disaggregate stage results into hourly ones. Desaggregating thermal generation is very easy, once in the proposed hourly model, as we do not consider thermal plant's typical constraints such as ramp and startup constraints, and, therefore, the generation of one hour does not depend on the previous hour generation.

In order to obtain the desaggregated thermal generation, we only need to recover the optimal position variable from the operation model. Then, for every stage, we perform the following calculation:

$$g^*_{j\tau} = \sum_l \lambda^*_l \hat{g}^l_{j\tau}, \forall \tau \in \mathcal{T}, j \in J \tag{5-12}$$

Where $\hat{g}^l_{j\tau}$ is the generation of plant j at hour τ when the hydroelectric plant is in the l^{th} position. This is a subproduct of the immediate cost function pre-calculation.

As the piecewise linear (or hyperplane) representation does not involve λ_l, its optimal value would have to be calculated. It is possible to obtain it by finding which beta constraint (equation 4-14) are biding in the optimal problem solution.

There is also a similar equation to obtain hydroelectric plants' hourly dispatches:

$$\phi_i = \frac{\rho_i u^*_i}{e^*}, \forall i \in I \tag{5-13}$$

$$e^*_\tau = \sum_l \lambda^*_l \hat{e}^l_\tau, \forall \tau \in \mathcal{T} \tag{5-14}$$

$$e^*_{i\tau} = \phi_i e^*_\tau, \forall i \in I, \tau \in \mathcal{T} \tag{5-15}$$

Where e^*, λ^*_l and u^*_i are the optimal results obtained when solving the immediate cost problem and $\hat{e}^l_\tau$ is also a subproduct of the immediate cost function calculation.

Clearly, as hydroelectric plants' generation depend on the amount of inflow of each hour and reservoir levels to generate, this approach does not always achieve a feasible solution. Using optimization to disaggregate hydroelectric hourly generations, although costlier computationally, always attain feasible solutions.

First, we performed the hourly disaggregation of the thermal plants. After that, since we have the total thermal generation and demand of each hour we know how much hydroelectric energy should be produced for each hour. To do so, we simply need to calculate:

$$e^*_\tau = d_t - \sum_j g^*_{tl}, \forall \tau \in \mathcal{T} \tag{5-16}$$

After obtaining the total hydroelectric energy per hour, for a given stage t, we need to solve the following optimization problem:

$$Min \sum_i (v_{i,t+1} - v^*_{i,t+1})^2 \tag{5-17}$$

$$v_{i,t+1} = v_{i,t} + \hat{a}_{t,i} + \sum_\tau -u_{i,\tau} - \nu_{i,\tau} + \sum_\tau \sum_{m \in U_i} (u_{m,\tau} + \nu_{m,\tau}), \forall i \in I \tag{5-18}$$

$$u_{i,\tau}\rho_i \leq \overline{e}_i, \forall i \in I, \tau \in \mathcal{T} \tag{5-19}$$

$$v_{i,t} \leq v_{imax}, \forall i \in I \tag{5-20}$$

$$v_{i,t} \geq v_{imin}, \forall i \in I \tag{5-21}$$

$$u_{i,\tau} \leq \overline{u}_i, \forall i \in I, \tau \in \mathcal{T} \tag{5-22}$$

$$\sum_i e_{i,\tau} = e^*_\tau, \forall \tau \in \mathcal{T} \tag{5-23}$$

$$v_{i,t+1}, u_{i,\tau} \geq 0, \forall i \in I, \tau \in \mathcal{T} \tag{5-24}$$

Where $v^*_{i,t+1}$ represent the optimal volume of hydroelectric plant i at the end of the current stage t.

Note that future and immediate cost functions are not necessary in this step, once the optimal hydroelectric generation is settled. The idea is to find a feasible point considering the hydroelectric generation constraints. Any feasible solution is acceptable as a disaggregation, as long as the hydroelectric final volumes are maintained. This is important because the future cost obtained in the execution of SDDP using the ICF is directly related to the final volume retrieved in the same problem and changing final volumes might affect the total cost of the solution.

5.2.3.2 Obtaining hourly marginal costs

One possible solution to address this matter would be to calculate the problem's optimal basis (and, therefore, dual variables' optimal values) from the optimal generation values calculated as shown in the previous section. Unfortunately, this type of calculation can be time consuming.

However, obtaining hourly marginal costs is crucial when it comes to decomposition schemes. For instance, it would be possible to create an investment model in which the sub-problem uses the ICF approach.

5.2.4
Computational challenges

As proposed before, the immediate cost representation has many great advantages. Unfortunately, as we increase the complexity of the graphs that need to be solved, the min cut problem grows exponentially. If we consider that we would have one extra node for each run-of-river water plant or battery, in addition to having to represent all stage hours in one single graph, we would have a very difficult problem.

In this case, enumerating cuts in no longer an option. One possible way to solve this problem is finding the graph's maximum flow which, as shown before, is equivalent to finding the minimum cut problem. The difference is that, in the sections above, as we were dealing with small graphs, cut enumeration was much more advantageous. However, as we increase the number of nodes and arcs, solving the maximum flow problem becomes more and more reasonable.

There are several max flow implementations that promise to solve maximum flow problems quickly, in several different programming languages. Julia, for instance, has an implementation based on Edmonds-Karp algorithm (17). Matlab has 2 max flow algorithm implementations: Edmonds-Karp and Goldberg's (18). R also relies on Goldberg's algorithm to solve max flow problems. There is also some literature on the implementation of such type of algorithms, such as (16).

Bibliography

[1] AURENHAMMER, F.. **Voronoi diagrams—a survey of a fundamental geometric data structure**. ACM Computing Surveys (CSUR), 23(3):345–405, 1991.

[2] AVIS, D.; FUKUDA, K.. **A pivoting algorithm for convex hulls and vertex enumeration of arrangements and polyhedra**. Discrete & Computational Geometry, 8(3):295–313, 1992.

[3] AVIS, D.; BREMNER, D.. **How good are convex hull algorithms?** In: PROCEEDINGS OF THE ELEVENTH ANNUAL SYMPOSIUM ON COMPUTATIONAL GEOMETRY, p. 20–28. ACM, 1995.

[4] BALERIAUX, H.; JAMOULLE, E.; DE GUERTECHIN, F. L. ; OTHERS. **Simulation de l'exploitation d'un parc de machines thermiques de production d'electricite couple a des stations de pompage**. Revue E, 5(7):225–245, 1967.

[5] BARBER, C. B.; DOBKIN, D. P. ; HUHDANPAA, H.. **The quickhull algorithm for convex hulls**. ACM Transactions on Mathematical Software (TOMS), 22(4):469–483, 1996.

[6] BENDERS, J. F.. **Partitioning procedures for solving mixed-variables programming problems**. Numerische mathematik, 4(1):238–252, 1962.

[7] BERTSEKAS, D. P.. **Dynamic programming and stochastic control**. 1976.

[8] BLOOM, J. A.; CHARNY, L.. **Long range generation planning with limited energy and storage plants part i: production costing**. IEEE transactions on power apparatus and systems, (9):2861–2870, 1983.

[9] BOOTH, R.. **Power system simulation model based on probability analysis**. IEEE Transactions on Power Apparatus and Systems, 1(PAS-91):62–69, 1972.

[10] CAMPODÓNICO, N.. **Representação analítica de falhas dos equipamentos e variação da demanda no despacho hidrotérmico multiestágio**. Tese de doutorado em engenharia de sistemas e computação, Universidade Federal do Rio de Janeiro, Rio de Janeiro, 1997.

[11] CARAMANIS, M.; STREMEL, J.; FLECK, W. ; DANIEL, S.. **Probabilistic production costing: an investigation of alternative algorithms**. International Journal of Electrical Power & Energy Systems, 5(2):75–86, 1983.

[12] CCEE. **Deck de preços**. www.ccee.org.br, 2016. Accessed in: March 2016.

[13] CLARKSON, K. L.; SHOR, P. W.. **Applications of random sampling in computational geometry, ii**. Discrete & Computational Geometry, 4(1):387–421, 1989.

[14] CRIE. **Informe anual 2015**. www.crie.org.gt, 2016. Accessed in: March 2016.

[15] DANTZIG, G. B.; WOLFE, P.. **Decomposition principle for linear programs**. Operations research, 8(1):101–111, 1960.

[16] DERIGS, U.; MEIER, W.. **Implementing goldberg's max-flow-algorithm—a computational investigation**. Zeitschrift für Operations Research, 33(6):383–403, 1989.

[17] EDMONDS, J.; KARP, R. M.. **Theoretical improvements in algorithmic efficiency for network flow problems**. Journal of the ACM (JACM), 19(2):248–264, 1972.

[18] GOLDBERG, A. V.; TARJAN, R. E.. **A new approach to the maximum-flow problem**. Journal of the ACM (JACM), 35(4):921–940, 1988.

[19] HELSETH, A.; BRAATEN, H.. **Efficient parallelization of the stochastic dual dynamic programming algorithm applied to hydropower scheduling**. Energies, 8(12):14287–14297, 2015.

[20] MACEIRA, M.; PEREIRA, M.. **Analytical modeling of chronological reservoir operation in probabilistic production costing [of hydrothermal power systems]**. IEEE transactions on power systems, 11(1):171–180, 1996.

[21] MCMULLEN, P.. **The maximum numbers of faces of a convex polytope**. Mathematika, 17(02):179–184, 1970.

[22] PAPADIMITRIOU, C. H.; STEIGLITZ, K.. **Combinatorial optimization: algorithms and complexity**. Courier Corporation, 1982.

[23] PEREIRA, M. V.; PINTO, L. M.. **Multi-stage stochastic optimization applied to energy planning**. Mathematical programming, 52(1-3):359–375, 1991.

[24] PEREIRA, M.. **Optimal stochastic operations scheduling of large hydroelectric systems**. International Journal of Electrical Power & Energy Systems, 11(3):161–169, 1989.

[25] POWELL, W. B.. **Approximate Dynamic Programming: Solving the curses of dimensionality**, volumen 703. John Wiley & Sons, 2007.

[26] PSR. **Stochastic dual dynamic programming. methodology manual**. www.psr-inc.com, 2016. Accessed in: January 2016.

[27] PSR. **Stochastic dual dynamic programming. user manual**. www.psr-inc.com, 2016. Accessed in: January 2016.

[28] PYHULL. **Pyhull documentation**. www.pythonhosted.org, 1995. Accessed in: November 2015.

[29] QHULL. **Read me**. www.qhull.org, 1995. Accessed in: November 2015.

[30] ROSS, S. M.. **Introduction to stochastic dynamic programming**. Academic press, 2014.

[31] WORLD BANK. **Electricity production from hydroelectric sources (% of total)**. www.data.worldbank.org, 2014. Accessed in: May 2016.

[32] YAKOWITZ, S.. **Dynamic programming applications in water resources**. Water resources research, 18(4):673–696, 1982.

6
Appendix A

6.1
SDP execution flow

SDP algorithm consists of enumerating all possible final volume states in order to approximate the future cost function (FCF) as well as possible. The algorithm is:

Algorithm 4 SDP algorithm

```
for each stage (last to first) do
  for each volume state do
    for each inflow scenario do
      Calculate minimum total operation cost (future + immediate)
    end for
    Calculate the average minimum cost
  end for
end for
```

Lastly, solve first stage problem considering the interpolated costs calculated in stage 2. As enumerating every possible volume state is impossible, we need to calculate future cost values for certain volume states and then interpolate them to obtain the future cost for other values.

Still, this approach might be expensive computationally once many problems will have to be solved so that the future cost function can be well approximated. For a hundred different value discretization (and disregarding inflow uncertainty), the number of problems solved per stage for a single reservoir would be 100. For 2 reservoirs, as they do not need to maintain same water levels would be 100^2 and so on. More examples can be seen in table 6.1.

# Reservoirs	# Combinations
1	100^1
2	$100^2 = 10.000$
3	$100^3 = 1.000.000$
4	$100^4 = 100.000.000$

5	$100^5 = 10.000.000.000$
6	$100^6 = 1.000.000.000.000$
50	$100^{50} = 1$ followed by 100 zeros

Table 6.1: Number of problems solved by number of reservoirs

7
Appendix B

7.1
SDDP execution flow

The figure 7.1 shows the main components of the operation problem for stage t, scenario s:

1. SDDP state variables at the beginning of the stage (in this example, initial storage v(t) and inflow along the stage, a(t));

2. reservoir storage balance equations, which determine the hydro turbined outflow, u(t);

3. power balance equation, which determines the least-cost operation of the thermal plants required to meet the residual load (after subtracting hydro generation and renewable production). In the SDDP formulation, the resulting operation cost is known as the immediate cost function (ICF);

4. future cost functions (FCF) l = 1,. . . ,L of the SDDP state variables for the next stage: the final storage v(t+1) and l = 1,. . . ,L conditioned inflow scenarios a(t+1,l).

5. the objective function is to minimize the sum of immediate cost ICF and the mean future cost $\frac{1}{L}\sum_l FCF_l$

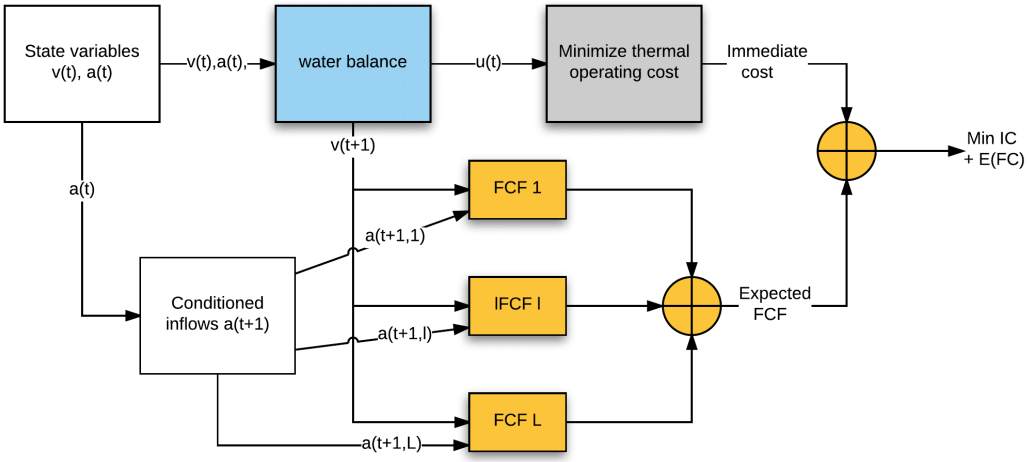

Figure 7.1: SDDP flowchart

In the following sections, SDDP algorithm phases will be described.

7.2 Backward recursion step

After the one-stage dispatch problem is solved, we generate a Benders (6) cut to improve the future cost function of the previous stage.

Assuming that the FCF for the previous stage already has $\mathcal{P}$ hyperplanes, the Benders cut will correspond to the $(\mathcal{P}+1)^{th}$ FCF constraint:

$$\alpha_t^l \geq \sum_i \hat{\varphi}_{t,i}^{h\mathcal{P}+1} \times v_{t,i} + \sum_i \hat{\varphi}_{t,i}^{a\mathcal{P}+1} \times a_{t,i}^l + \hat{\varphi}_t^{o\mathcal{P}+1} \tag{7-1a}$$

The Benders cut coefficients $\hat{\varphi}_{t,i}^{h\mathcal{P}+1}$, $\hat{\varphi}_{t,i}^{a\mathcal{P}+1}$ and $\hat{\varphi}_t^{o\mathcal{P}+1}$ are calculated from a linear expansion of the optimal solution α_t^* of the one-stage dispatch problem (1-1 - 1-10) (section 1.2).

$$\alpha_t\left(v_t, a_t\right) \approx \alpha_t^* + \sum_i \frac{\partial \alpha_t}{\partial v_{t,i}} \times \left(v_{t,i} - \hat{v}_{t,i}^s\right) + \sum_i \frac{\partial \alpha_t}{\partial a_{t,i}} \times \left(a_{t,i} - \hat{a}_{t,i}^s\right) \tag{7-1b}$$

The coefficient $\hat{\varphi}_{t,i}^{h\mathcal{P}+1}$ corresponds to $\frac{\partial \alpha_t}{\partial v_{t,i}}$, which is the simplex multiplier $\pi_{t,i}^h$. In turn, $\hat{\varphi}_{t,i}^{a\mathcal{P}+1}$ corresponds to $\frac{\partial \alpha_t}{\partial a_{t,i}}$, calculated as: $\pi_{t,i}^h + \left(\frac{\hat{\rho}_{t,i}}{\hat{\sigma}_{t,i}}\right) \times \pi_{t,i}^a$. Finally, the constant term is obtained by adding all the constants of the linear expansion:

$$\hat{\varphi}_t^{o\mathcal{P}+1} = \alpha_t^* - \sum_i \hat{\varphi}_{t,i}^{h\mathcal{P}+1} \hat{v}_{t,i}^s - \sum_i \hat{\varphi}_{t,i}^{a\mathcal{P}+1} \hat{a}_{t,i}^s \tag{7-1c}$$

7.3 Forward simulation step

7.3.1 Upper bound calculation

In stage t, scenario s of the forward simulation step, we calculate the immediate operation cost associated to optimal solution (indicated by the superscript "*").

$$z_t^s = \sum_j c_j \sum_\tau g_{t,\tau,j}^* \tag{7-2a}$$

As in the traditional SDDP formulation, the upper bound is calculated as:

$$\overline{z} = \frac{1}{S} \sum_t \sum_s z_t^s \tag{7-2b}$$

7.3.2 Inflow vector for stage t + 1. scenario s

We also calculate in the forward simulation step the inflow scenario vector for the next stage $t+1$: $\left\{\hat{a}_{t+1,i}^s,\ i = 1,\ \ldots,\ I\right\}$. This is done by sampling from the expression for the conditioned inflows, equation 7-2c:

$$\frac{\left(a_{t+1,i}^l - \hat{\mu}_{t+1,i}\right)}{\hat{\sigma}_{t+1,i}} = \hat{\rho}_{t,i} \times \frac{\left(\hat{a}_{t,i}^s - \hat{\mu}_{t,i}\right)}{\hat{\sigma}_{t,i}} + \sqrt{1 - \hat{\rho}_{t,i}^2} \times \xi_{t,i}^l \quad \forall l = 1, \ldots, L;\ \forall i = 1, \ldots, I \tag{7-2c}$$

Basically, $\hat{s}$ is uniformily sampled from the set $\{1, \ldots,\ L\}$, and the inflows $\left\{\hat{a}_{\mathrm{ti}}^{\hat{s}},\ i = 1,\ \ldots,\ I\right\}$ are calculated for the corresponding innovation vector $\left\{\hat{\xi}_{t,i}^{\hat{s}},\ i = 1,\ \ldots,\ I\right\}$. Note that the entire innovation vector has to be used in order to preserve the spatial correlation.

$$\frac{\left(a_{t+1,i}^{\hat{s}} - \hat{\mu}_{t+1,i}\right)}{\hat{\sigma}_{t+1,i}} = \hat{\rho}_{t,i} \times \frac{\left(\hat{a}_{t,i}^s - \hat{\mu}_{t,i}\right)}{\hat{\sigma}_{t,i}} + \sqrt{1 - \hat{\rho}_{t,i}^2} \times \hat{\xi}_{t,i}^{\hat{s}} \quad \forall i = 1, \ldots, I \tag{7-2d}$$

Further informations can be obtained in (26).

7.3.3 SDDP parallel execution

Currently, SDDP parallelization is performed considering time synchronicity. All figures in this section were extracted from (27). Figure 7.2 illustrates how forward phase is parallelized. Each forward scenario is solved by a single processor until every scenario is solved for a certain stage t. After that, stage t+1 scenarios start to be solved.

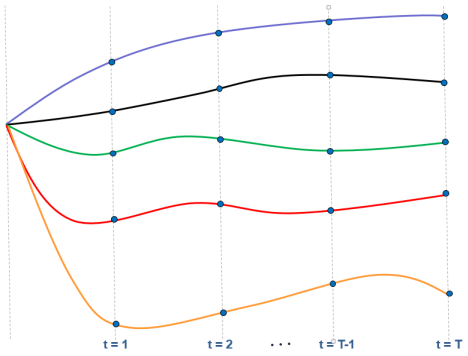

Figure 7.2: SDDP forward step parallelization

Figure 7.3 illustrates how backward phase is parallelized. All backward scenarios from a certain stage t are solved by the same process. After all backwards from stage t are solved, stage t-1 scenarios start to be solved.

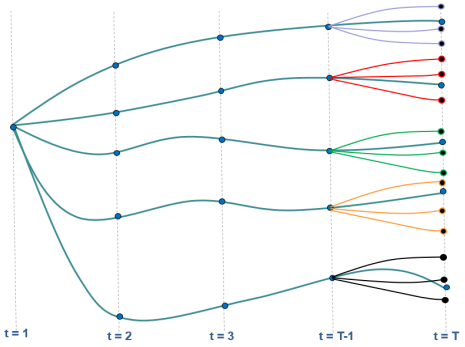

Figure 7.3: SDDP backward step parallelization

8
Appendix C

8.1
Proof of equality between hydro opportunity costs

Let us consider the following dispatch optimization problem:

$$\alpha_t(\hat{v}_t) = Min \sum_j c_j g_{t,j} + \alpha_{t+1}(v_{t+1}) \tag{8-1}$$

$$\sum_i e_{t,i} + \sum_j g_{t,j} = \hat{\delta}_t \quad \leftarrow \pi_{d_t} \tag{8-2}$$

$$e_{t,i} = \rho_i u_{t,i} \quad \leftarrow \pi_{e_{t,i}} \quad \forall i \in I \tag{8-3}$$

$$v_{t+1,i} = \hat{v}_{t,i} + \hat{a}_{t,i} - u_{t,i} - \nu_{t,i} + \sum_{m \in U_i} (u_{t,m} + \nu_{t,m}) \quad \leftarrow \pi_{h_{t,i}} \quad \forall i \in I \tag{8-4}$$

$$g_{t,j} \leq \overline{g}_j \quad \leftarrow \pi_{g_{t,j}} \quad \forall j \in J \tag{8-5}$$

$$v_{t+1,i} \leq \overline{v}_i \quad \leftarrow \pi_{v_{t,i}} \quad \forall i \in I \tag{8-6}$$

$$u_{t,i} \leq \overline{u}_i \quad \leftarrow \pi_{u_{t,i}} \quad \forall i \in I \tag{8-7}$$

$$\alpha_{t+1} \geq \sum_i \hat{\phi}^p_{t+1,i} \times v_{t+1,i} + \hat{\sigma}^p_{t+1} \quad \leftarrow \pi_{c_{t,p}} \quad \forall p \in P \tag{8-8}$$

Where variable $e_{t,i}$ is unbounded and all other variables are greater or equal to zero.

The dual constraint related to $e_{t,i}$ (considering that the variable is unbounded) is:

$$\pi_{e_{t,i}} + \pi_{d_t} = 0, \forall i \in I \tag{8-9}$$

The dual constraint related to $u_{t,i}$ is:

$$-\rho_i \pi_{e_{t,i}} + \pi_{h_{t,i}} - \pi_{h_{t,k}} + \pi_{u_{t,i}} \leq 0, \forall i \in I \tag{8-10}$$

Where $\pi_{h_{t,k}}$ is the dual variable associated with the water balance constraint of the downstream plant of hydro i (hydro k)

On the other hand, if we consider $u_{t,i} > 0$, by the complementary slackness condition, we know that:

$$-\rho_i \pi_{e_{t,i}} + \pi_{h_{t,i}} - \pi_{h_{t,k}} + \pi_{u_{t,i}} = 0, \forall i \in I \tag{8-11}$$

If we consider that no hydroelectric plant is turbined at its maximum capacity ($u_{t,i} < \overline{u}_i$, that is, $\pi_{u_{t,i}} = 0$) then:

$$\pi_{e_{t,i}} = \frac{\pi_{h_{t,i}} - \pi_{h_{t,k}}}{\rho_i}, \forall i \in I \tag{8-12}$$

Which is exactly the formula of the hydroelectric opportunity cost. In other words, if the hydroelectric plants do not hit turbine limits, i.e. do not turbine at all or turbine at its maximum capacity, we know that all hydroelectric opportunity costs are equal.